

**Simultaneous Measurement of Blood Flow and Oxygen Consumption
Immediately Post-Exercise with Magnetic Resonance Imaging**

by

Kory Wallace Mathewson

A thesis submitted in partial fulfillment of the requirements for the degree of

Master of Science

Department of Biomedical Engineering
University of Alberta

© Kory Wallace Mathewson, 2014

Abstract

Maximal pulmonary oxygen uptake (pulmonary VO_2max), which is equal to the product of cardiac output and arterial-venous oxygen content difference, is the gold standard measure of aerobic fitness. This test is used routinely in studies of exercise physiology and clinic research, particularly in the study of heart failure. A limitation of pulmonary VO_2 measurement during whole body exercise is that it integrates all factors that determine oxygen consumption, including oxygen transport and oxygen utilization by active muscles. Thus, this test cannot distinguish oxygen delivery or extraction limitations of the exercising muscle independently. Currently, there is no non-invasive method for simultaneously measuring skeletal muscle oxygen consumption and its determinants (muscle blood flow and muscle oxygen extraction) during dynamic exercise, which is necessary to expose the mechanisms of dysfunction along the oxygen cascade in health and disease.

In this thesis, I propose a new imaging approach which interleaves complex-difference (CD) and susceptometry magnetic resonance imaging (MRI) pulse sequences for real-time imaging of venous blood flow (VBF) and venous oxygen saturation (SvO_2) for the calculation of skeletal muscle oxygen consumption (VO_2). The goals of this thesis were to develop the imaging method, with specific targeting of the femoral vein and quadriceps muscle group, and to determine the reproducibility of this novel approach during sub-maximal single-leg knee-extensor (SLKE) exercise.

When combined with cardiac and vascular studies, these non-invasive methods provide necessary tools to investigate the relative contributions of the mechanisms that reduce exercise capacity in those at risk for, or with, heart failure.

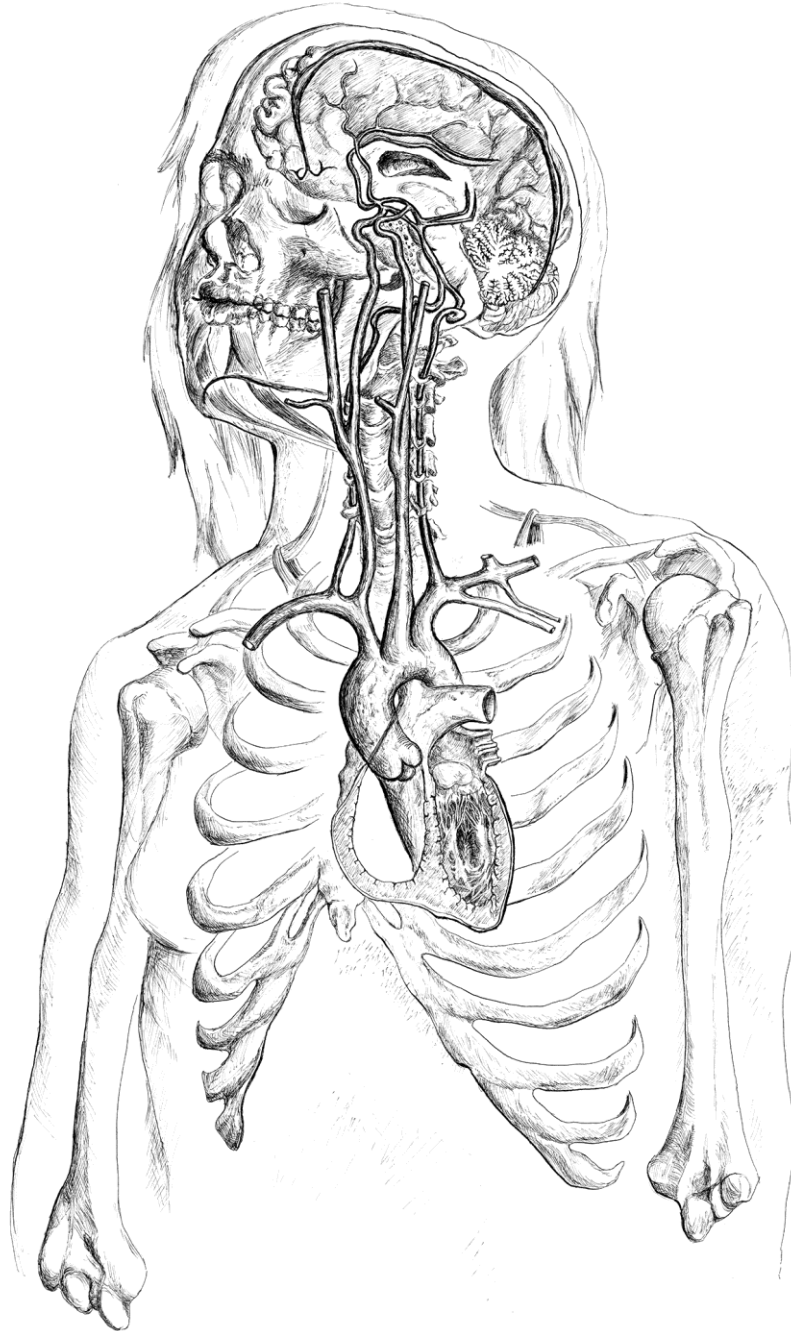
Preface

This thesis is an original work by Kory Mathewson. The main research project, of which this thesis is a component, received research ethics approval from the University of Alberta Research Ethics Board: Skeletal muscle blood flow across the heart failure continuum, No. Pro00040073.

The literature review in Chapter 1, the manuscript in Chapter 2, and the concluding analysis in Chapter 3 are original work. Chapter 2 of this thesis has been submitted for publication consideration to *Magnetic Resonance in Medicine as Mathewson KW, Haykowsky MJ, Thompson RB. Feasibility and Reproducibility of Measurement of Whole Muscle Blood Flow, Oxygen Extraction and VO₂ with Dynamic Exercise Using MRI. (submitted August 2014)*. I was responsible for the data extraction from the collected data, the data analysis, as well as the manuscript preparation. The technical apparatus referred to in Chapter 2 was conceptualized, designed, and built with the assistance of Robert Lederer, Associate Professor in Design Studies at the University of Alberta. Dr. Mark Haykowsky assisted with the data collection and analysis, provided a physiological context for the research project, and contributed to manuscript writing and editing. Dr. Richard B. Thompson is the supervisory author on the manuscript; he performed the MRI scan experiments, assisted with the data collection and analysis, and aided in writing the manuscript.

Dedication

This thesis is dedicated to the advancement of medical science technologies for the betterment of the understanding of human health.



Sandy Escobar

Acknowledgements

The incredible support and motivation from an entire community of individuals has made this thesis, and the last three years of research in the pursuit of a graduate degree in Biomedical Engineering, possible.

Thank you to my supervisor, Dr. Richard Thompson. You are a wonderful motivator and teacher. The process through which you break down complex concepts and make them understandable is incomparable. I appreciate your care and dedication to my personal growth and our research. I would also like to thank Dr. Mark Haykowsky for being a supervisory committee member for this thesis work. You have nurtured and helped develop my passion for physiological research. Thank you for your dedicated hours of support and for pushing me to maximize my VO_2 . Thank you to Dr. Alan Wilman, the third member of my supervisory committee, for providing an external eye on my research and helping push me along, and stay on track. Thank you to Robert Lederer, your skill and talent in the design and fabrication of MRI compatible devices is unparalleled. You are an inspiration and a craft master, and it has been a pleasure working with you.

I would like to acknowledge the financial support from the Department of Biomedical Engineering, the Faculty of Medicine and Dentistry and the University of Alberta. Thank you to the Faculty of Graduate Studies and Research and the Graduate Students' Association for travel funding. As well, for providing financial support to Dr. Richard B. Thompson's laboratory, I would like to express gratitude to the Alberta Heart Failure Etiology and Analysis Research Team (Alberta HEART) team grant, Alberta Innovates Health Solutions (AIHS), and the Canadian Institute of Health Research (CIHR).

It is with delight that I am able to acknowledge the conferences at which I was invited to present my research. They include the 2014 International Society for Magnetic Resonance in Medicine Joint Annual Meeting in Milan, Italy, the 2013 Alberta Imaging Symposium in Calgary, Alberta, the 2013 Re: Engineering

Leadership Consortium, as well as the 2012 and 2014 Faculty of Engineering Graduate Research Symposiums in Edmonton, Alberta.

My lab group has been an incredible source of support and honest, sincere critique. Those peers that I have worked with most closely include Kelvin Chow, Joseph Pagano, June Cheng Baron, and Sarah Theisson. Thank you for the countless scans, the brain busting code challenges, and the fun. Also, sincere gratitude to all the volunteers who contributed their body and their time in the name of science by allowing me to scan what is happening inside their bodies while being encouraged to exercise.

Thank you to the Office of the Dean of Students at the University of Alberta for making possible my extracurricular endeavors over the course of my graduate and undergraduate degree programs. Thank you to my wonderful family from Rapid Fire Theatre, the Varscona Theatre, and across the world in all areas of improvisational theatre. You have made life worth living over the last ten years. With such a focus on improvisation, it is hard to imagine that something so concrete came out of this mind.

This thesis and the last several years of my life would not have been possible without the best brothers in the world, Kyle and Keyfer. You guys rule. Michele and Bruce, you made me and then I made this, so by proxy you made this.

Finally, Mufty and Bill, you are my inspiration.

Table of Contents

Abstract.....	ii
Preface.....	iii
Dedication.....	iv
Acknowledgements.....	v
List of Figures and Tables.....	ix
List of Abbreviations and Symbols.....	x
Chapter 1: Introduction and Background.....	1
Introduction.....	1
Background.....	1
Blood Flow, Oxygen Extraction and Oxygen Consumption.....	2
Blood Flow.....	3
Oxygen Extraction.....	4
Oxygen Consumption.....	5
Exercise Stress.....	6
Measuring Blood Flow, Oxygen Extraction and Oxygen Consumption.....	7
Invasive Techniques to Measure Oxygen Consumption.....	8
Non-invasive Techniques.....	9
Doppler Ultrasound.....	9
Near-Infrared Spectroscopy (NIRS).....	10
Positron Emission Tomography (PET).....	10
MRI Techniques.....	11
Exercise in the MRI.....	20
Scope of Thesis.....	21
Chapter 1 References.....	24
Chapter 2: Feasibility and Reproducibility of Measurement of Skeletal Muscle Blood Flow, Oxygen Extraction and VO ₂ with Dynamic Exercise Using MRI..	35
Introduction.....	35
Methods.....	37
Subjects.....	37
Exercise Device.....	37

Imaging of Venous Oxygen Saturation	38
Complex-difference Flow Imaging for Estimation of Venous Blood Flow (VBF).....	40
Pulse Sequence	43
Exercise and Imaging Protocol.....	44
Measurement of Skeletal Muscle Oxygen Consumption	47
Vessel Tilt Calculation	47
Reproducibility and Statistical Analysis.....	48
Results	48
Discussion	52
Experimental Considerations.....	55
Limitations.....	56
Conclusion.....	57
Chapter 2 References	59
Chapter 3: Discussion and Conclusions.....	63
Introduction and General Findings.....	63
Limitations and Future Directions.....	63
Conclusions	65
Chapter 3 References	66

List of Figures and Tables

Figure 1.1 – Velocity encoding with first moments	12
Figure 1.2 – Phase contrast and complex difference comparison	15
Figure 2.1 – Pulse sequence schematic	39
Figure 2.2 – Complex-difference imaging example	42
Figure 2.3 – Exercise study protocol	44
Figure 2.4 – Imaging location	45
Figure 2.5 – Slice-prescription details	46
Figure 2.6 – Sample imaging results	49
Figure 2.7 – Test re-test group average data	50
Table 2.1 – Group mean data	51
Figure 2.8 – Test re-test correlations	54
Figure 2.9 – Muscle mass correlations	54

List of Abbreviations and Symbols

2D	Two-dimensional
3D	Three-dimension
A	Area of a blood vessel
a-vO₂ diff	Arteriovenous oxygen difference
B₀	Main magnetic field strength
BF	Blood flow
BOLD	Blood-oxygen-level-dependent
Ca	Oxygen carrying capacity
CaO₂	Arterial oxygen content
CD	Complex difference
CD-MRI	Complex difference magnetic resonance imaging
χ	Magnetic susceptibility
CvO₂	Venous oxygen content
ΔB	Change in main magnetic field
$\Delta\chi$	Difference in magnetic susceptibility
$\Delta\chi_{[do]}$	Susceptibility difference between oxygenated and deoxygenated blood
ΔHbO_2	Deoxyhemoglobin
ΔM_1	Change in the first magnetic moment
$\Delta\phi$	Difference in phase
ΔTE	Echo-time spacing
EDV	End-diastolic volume
EF	Ejection fraction
ESV	End-systolic volume
Fe²⁺	Iron ion
γ	Gyromagnetic ratio
$\gamma(^1H)$	Gyromagnetic ratio for a proton, VALUE
GRE	Gradient-echo
HbO₂	Oxyhemoglobin
Hct	Hematocrit
HF	Heart failure
Hgb	Hemoglobin
HR	Heart rate
KE	Knee extension exercise
MR	Magnetic resonance
MRI	Magnetic Resonance Imaging
NIRS	Near-infrared spectroscopy
O₂	Oxygen
PC	Phase contrast
PC-MRI	Phase-contrast magnetic resonance imaging

PET	Positron emission tomography
Q	Cardiac output
Q_{fv}	Blood flow in the femoral vessel
RF	Radio frequency
ROI	Region of interest
SaO₂	Arterial oxygen saturation
SD	Standard deviation
SLKE	Single leg knee extension
SMBF	Skeletal muscle blood flow
SV	Stroke volume
SvO₂	Venous oxygen saturation
T	Tesla, unit of magnetic field strength
T1	Longitudinal, spin-lattice relaxation time
T2	Transverse, spin-spin relaxation time
T2*	Effective transverse relaxation time, $1/T2' + 1/T2 = 1/T2^*$
T2'	Transverse relaxation due to magnetic field inhomogeneities, chemical shift of the second kind and induced magnetic susceptibilities
TE	Echo time
θ	Angle between the vessel of interest and B ₀
TRUST	T2-relaxation-under-spin-tagging
v	Velocity of blood flow in phase contrast
VENC	Encoding velocity
VO₂	Oxygen consumption
VO_{2(KE)}	Oxygen consumption in a knee extension exercise
VO_{2max}	Maximal whole body oxygen consumption
VO_{2muscle}	Oxygen consumption in working muscle

Chapter 1: Introduction and Background

Introduction

During exercise stress, metabolic demand and oxygen delivery are strongly coupled. The intensity of skeletal muscle contractions is correlated to oxidative metabolism and skeletal muscle blood flow. Simultaneous quantification of the factors contributing to muscle oxygen consumption (VO_2), explicitly blood flow, and oxygen extraction can elucidate disease states and refine treatment. This relationship is particularly significant during and immediately post-exercise.

Patients with, or at risk for, heart failure exhibit decreased peak oxygen (O_2) consumption and impaired biomechanical efficiency (external work performed divided by oxygen consumption) during exercise when compared to healthy controls (1, 2). Patients with heart failure consume more oxygen relative to their healthy, age-matched controls to perform similar levels of activity and the amount of additional oxygen required increases with the severity of the heart failure (3, 4).

Exercise intolerance in patients with heart failure and those at risk for heart failure (e.g. diabetes and obesity) may be due to restricted blood flow, maximal muscle oxygen consumption limitations, or some combination of factors. Independent impairments in the components of the muscle oxygen consumption may be elucidated with investigation before, during, and immediately following dynamic exercise. Safe and robust methods to simultaneously quantify blood flow and oxygen extraction, which determine the resulting muscle oxygen consumption in the exercising muscle, are needed to understand disease mechanisms and evaluate treatment.

Background

Heart Failure (HF) occurs when the heart is unable to supply sufficient blood flow to meet the demands of the body (5). HF is the most-common heart disease. A poor understanding of the mechanisms of heart failure and how to treat

the underlying causes means that many patients will not respond to therapy (6, 7). There are an estimated 500,000 Canadians living with heart failure, and 50,000 new patients are diagnosed every year (8). Almost 50% of people with heart failure die within 5 years of diagnosis (9). By making an accurate and timely diagnosis and tracking disease progression, early intervention (e.g. pharmacological, lifestyle, etc.) could be initiated to reduce risk factors, symptoms, and hospitalizations and improve quality of life and prolong survival (6).

While exercise intolerance is a cardinal feature of heart failure, it is prevalent in a number of common disease states including diabetes, obesity, cancer, and muscular dystrophy. In all of these pathologies, the exercise intolerance may be due to reduced blood flow, impaired oxygen extraction, or a combination of factors. If independent impairments and limitations of the factors that contribute to muscle oxygen consumption can be measured, targeted therapies can potentially be prescribed on an individual basis.

Blood Flow, Oxygen Extraction and Oxygen Consumption

Three main systems compose the human cardiovascular system: bronchial circulation, systemic circulation, and pulmonary circulation. The bronchial circulation supplies blood to the tissues of the large airways of the lungs. The systemic circulation carries oxygenated, or oxygen-rich, blood from the heart to the body and returns deoxygenated blood to the heart. The pulmonary circulation system carries deoxygenated blood from the heart to the lungs, where the blood can release carbon dioxide and pickup oxygen during respiration, and then returns oxygenated blood back to the heart from the lungs. The pickup of oxygen during respiration is made possible by hemoglobin.

The oxygen rich arterial blood carries oxygen that is chemically combined with hemoglobin (10). Four protein subunits, each containing a ferrous (Fe^{2+}) ion, compose a single hemoglobin unit. The average hemoglobin level for males is 14 to 18 g/dl and for females is 12 to 16 g/dl (10, 11). Hematocrit is the volume

percentage of red blood cells in the blood. The normal hematocrit for men is 40 to 54%; for women it is 36 to 48% (11).

Hemoglobin has an oxygen carrying capacity (Ca) of 1.34-1.37 ml O₂ per gram hemoglobin (12). The oxygen carrying capacity of a gram of hemoglobin multiplied by the concentration of hemoglobin in the blood provides a measure of how effectively an individual can carry oxygen to working tissue. A blood draw is often used to measure this carrying capacity and it has been shown to be constant during exercise (13-16).

The blood flow through the pulmonary and systemic circulatory systems is responsible for the oxygenation of blood and the delivery of that oxygenated blood around the body and to working muscle tissue. When studying oxygen consumption and blood flow, the mass of the investigated tissue is of critical importance as these variables are often expressed per unit mass to provide comparable normalized values (17, 18). Blood flow, oxygen saturation in the blood, and oxygen consumption by the working tissue are all explored below, providing additional context for the physiologic parameters of interest.

Blood Flow

Under normal resting conditions, the heart can maintain a healthy supply of blood to every part of the body. Cardiac output (Q) is the amount of blood flow pumped by a single ventricle of the heart in one minute. An average resting cardiac output would be 4.9 L/min for a female and 5.6 L/min for a male (19). Cardiac output is often expressed as the product of the heart rate and stroke volume, the volume of blood pumped from one ventricle of the heart with each beat:

$$Q = HR * SV \qquad \text{Eq. 1.1}$$

In Eq. 1.1, Q is the cardiac output, HR is the heart rate of the individual measured in beats per minute, and SV is the stroke volume, the volume of blood pumped from one ventricle of the heart with each beat. A value for stroke volume can be obtained by subtracting the end-systolic volume (ESV), the volume of blood

in the ventricle at the end of a contraction, from the end-diastolic volume (EDV), the volume of blood in a ventricle at the end of filling in.

$$SV = EDV - ESV \quad \text{Eq. 1.2}$$

During exercise, both the heart rate and the stroke volume may increase, thereby increasing the cardiac output. In a healthy individual, most of the increase can be attributed to an increase in heart rate. Stroke volume depends on several factors such as heart size, contractility, duration of contraction, preload, and afterload. Other factors that act to increase cardiac output include the following: the skeletal muscle pump, increased depth and frequency of breathing, and venous tone, and decreased peripheral resistance. There are physiological limits to stroke volume and heart rate that can both limit maximal cardiac output. In some healthy, trained athletes maximal cardiac output can reach 42.3 L/min (20).

The fundamental characteristic of heart failure is the inability for the heart to provide sufficient blood flow to supply the needs of the body (5). In many pathologies blood flow to particular working muscle groups is obstructed or otherwise limited (e.g. peripheral vascular disease). An understanding of local blood flow to working tissue can help elucidate contributions of blood flow limitations to maximal oxygen consumption in a muscle. Blood flow may not be the only limiting factor; oxygen consumption may also be limited by oxygen extraction, or how much oxygen is removed from the blood as it passes through the capillaries.

Oxygen Extraction

Arteriovenous oxygen difference (a-vO₂ diff) is the change in oxygen content of the arterial and the venous blood, indicating how much oxygen was removed from the blood by the capillaries during circulation. The arteriovenous difference is measured by comparing the difference in the oxygen saturation of oxygenated, arterial blood (SaO₂) and the oxygen saturation of venous, deoxygenated blood (SvO₂). SaO₂ is relatively straightforward to measure using a

pulse oximeter, and the arterial oxygen saturation remains constant with exercise (16) except in some cases of endurance-trained athletes performing intense exercise (21).

$$a-vO_2 \text{ diff} = Ca * (SaO_2 - SvO_2) \quad \text{Eq. 1.3}$$

Eq. 1.3 shows that the a-vO₂ diff is calculated by multiplying the difference in saturation of arterial and venous blood by the oxygen-carrying capacity of the blood (Ca). Usually, the a-vO₂ diff is described in units of mL O₂ / 100 mL blood.

There are several pathologies where the oxygen-carrying capacity of the blood decreases, such as anemic hypoxia or hystotoxic hypoxia (22). Understanding the extraction of the oxygen from the blood provides insight into the contributions of oxygen consumption in working muscle tissue. By characterizing constraints in the blood flow, and the oxygen extraction, oxygen consumption in working tissue can be more fully described, and limitations can be fully elucidated.

Oxygen Consumption

Whole body maximal oxygen consumption (VO_{2max}) serves as the primary measure of exercise capacity. The arteriovenous oxygen difference and the cardiac output are the main factors that determine the variation in the body's total oxygen consumption. VO_{2max} is commonly quantified by measuring the oxygen concentration in expired air at the peak workload in a graded exercise stress test in which intensity is progressively increased. VO_{2max} is reached when the oxygen consumption remains steady despite an increase in workload. VO_{2max} is defined by the Fick equation:

$$VO_{2max} = Q * (CaO_2 - CvO_2) \quad \text{Eq. 1.4}$$

These values must be obtained during exertion at maximal effort. In Eq. 1.4 Q is the cardiac output, CaO₂ is the arterial oxygen content, and CvO₂ is the venous oxygen content. Whole body VO₂ testing cannot provide a local measure of skeletal muscle oxygen consumption (23). Local muscle oxygen consumption can be

estimated using Fick's principle by measuring blood flow to the muscle together with the muscle's arterial and venous blood oxygen saturations (24):

$$VO_{2\text{muscle}} = Ca * Q * (SaO_2 - SvO_2) \quad \text{Eq. 1.5}$$

The $VO_{2\text{muscle}}$ is calculated as the product of the carrying capacity of hemoglobin (Ca), the blood flow to the muscle (Q), and the difference between the saturation of fully oxygenated blood in the artery feeding the muscle (SaO_2) and the partially desaturated deoxygenated blood returning from the muscle in the veins (SvO_2). At rest, the usual range of SvO_2 is 50-75% (25), and the average values for SaO_2 are in the range of 97-99% (26, 27). While Q is often measured as arterial blood flow (locally or whole body), Q can also be measured on the venous return side (28, 29).

The amount of oxygen delivered to the tissue is dependent on several parameters including the metabolic demand, arterial oxygen content, rate of blood flow, temperature, and hematocrit (Hct) (10). By measuring the oxygen consumption, we can characterize the limitations to exercise in patients with, or at-risk for, heart failure. Measuring blood flow, oxygen saturation, and thus oxygen consumption at rest provides an understanding of the basal oxygen metabolism, but to truly understand the effects of potential limitations we need to push the limits by introducing a stress to the system.

Exercise Stress

Exercise stress testing is an essential tool in the detection and treatment of heart disease. Physical exertion is preferred to pharmacological testing because it links physical activity to symptoms (30). In addition, side effects are a potential disadvantage of pharmacological testing. The cardiopulmonary exercise testing is useful for assessing therapy and stratifying risk in patients with heart failure (31-33). A fundamental characteristic of heart failure is an impaired ability to increase cardiac output appropriately with exercise (34, 35).

Exercise is associated with a number of physiologic changes, including an increase in cardiac output from a resting value of 5 L/min to as much as 42.3 L/min. (20, 29, 36, 37). During exercise both the heart rate and the stroke volume may increase, thereby increasing the cardiac output. Hemodynamic phenomenon may be hidden during rest, especially for sedentary individuals, and an exercise challenge may help to induce hemodynamic changes, thereby elucidating differences between healthy and disease states.

When compared to rest, exercise induces a marked increase in oxygen consumption, cardiac output (CO), heart rate (HR), ejection fraction (EF), and stroke volume (SV) (38). Exercise significantly increases oxygen demand of muscle when compared to rest. This increased distribution to muscle cells may induce hypoperfusion in other organs (39, 40). During physical exercise at 50% heart rate acceleration, Weber et al. observed an increase in aortic and pulmonary flow during exercise (41). Cheng et al. measured a similar increase of the flow volume in the main pulmonary artery (42). Exercise stress increases the blood flow delivered to the tissue and the oxygen extraction of the tissue. During peak exercise venous oxygen saturation drops significantly and maximal oxygen uptake can be characterized.

Measuring Blood Flow, Oxygen Extraction and Oxygen Consumption

Whole body oxygen consumption reflects the aerobic physical fitness of an individual, but it may not correlate to local muscle tissue oxygen consumption, and it cannot provide any measure of the local muscle blood flow or local tissue oxygen saturation. While tissue oxygen saturation is directly measurable with several imaging modalities discussed below, the techniques have limitations. Local tissue saturation can be estimated by the blood oxygen saturation in the vessels draining from that tissue (10). Quantitatively measuring local tissue oxygen saturation is important to describe the physiological and pathological state of muscle function (43). Simultaneous measurement of the physiological contributions to muscle

oxygen consumption is critical to elucidate independent impairments in flow or oxygen extraction.

There are invasive and non-invasive methods to measure blood flow, oxygen extraction, and oxygen consumption. Invasive techniques involving catheterization include large vein oximetry. Some techniques, including flow measurement by the ^{133}Xe -washout method, utilize an injected radioactive tracer and invasive catheterization. Others techniques utilize ionizing radiation such as positron emission tomography (PET), single photon emission computed tomography (SPECT), or Xenon computer tomography (Xenon CT). Non-invasive techniques that do not use ionizing radiation such as Doppler ultrasound (US), near-infrared spectroscopy (NIRS) and magnetic resonance imaging (MRI) are preferable. The use of these invasive and non-invasive methods in previous studies for the measurement of blood flow, oxygen extraction, and oxygen saturation are explored below. Several imaging modalities have been used to measure simultaneous blood flow and muscle oxygen consumption changes in response to exercise stress. Our newly developed MRI technique is also briefly described below. The feasibility and reproducibility of the new method are detailed completely in Chapter 2.

Invasive Techniques to Measure Oxygen Consumption

In the late 1940's, Kety and Schmidt devised a method to measure regional blood flow invasively based on the principle that the rate at which an inert gas concentration in the venous circulation approaches the concentration in the arterial circulation is dependent on the volume of blood flowing through the tissue (45-47). This fundamental principle has led to measuring blood flow by administering an inert radioisotope, commonly ^{133}Xe , and monitoring clearance of the radioisotope using sensitive detectors. Oximetry involves the catheterization of the jugular vein and must be paired with flow measurement with Doppler ultrasonography to garner information on oxygen consumption (10, 48).

Resting femoral venous blood flow (Q_{fv}) between 0.15-0.40 L/min was measured using the thermodilution technique. No-load knee extension exercise increased Q_{fv} to an average value of 1.45 L/min; Q_{fv} increased linearly, as work rate increased, to a maximal flow of 6.21 L/min (29). Andersen and Saltin measured a resting femoral venous blood oxygenation (S_vO_2) of 70-75% and a no-load knee-extension exercise S_vO_2 of 40% (29). They also found that S_vO_2 decreased linearly with an increase in work rate (29). At a maximal work rate averaging 60W they measured an S_vO_2 of 24-29% (29). Knee extensor oxygen uptake, $VO_{2(K.E)}$, was measured between 6-12 ml/min at rest and no-load knee extension exercise increased $VO_{2(K.E)}$ to 0.191 L/min. $VO_{2(K.E)}$ increased linearly as work rate increased to maximum values of 0.52 – 0.76 L/min for sedentary individuals and 1.0 L/min in very fit subjects (29). Andersen and Saltin showed a peak oxygen uptake in limb skeletal muscle from 0.2-0.4 L/min/kg. A muscle mass of only 10-15kg was involved to elicit maximal oxygen consumption in a muscle (29, 49). When arm exercise was added to maximal leg exercise, maximum oxygen consumption values increased. These increases had a proportionally greater dependence on the increase in arteriovenous oxygen difference than on the cardiac output.

Invasive methods may measure changes in blood flow, oxygen saturation and oxygen extraction in response to exercise, but there are several disadvantages including discomfort of the patient due to the catheterization, long data acquisition, and inherently low temporal resolution due to the blood draw time (29, 37, 48). Accurate, easy to perform noninvasive measurements of blood flow, oxygen saturation, and oxygen extraction are preferable to invasive methods for several reasons including less likelihood of complication and a reduced dependence on operator experience (10, 50).

Non-invasive Techniques

Doppler Ultrasound

Doppler ultrasound can be used to measure blood flow faster than other imaging modalities. It is a non-invasive, non-radiating measurement technique

where the mean flow in the center of the vessel is represented by the maximal frequency of the Doppler shift (51, 52). The technique estimates blood flow velocity based on two major assumptions: a constant diameter of the insonated vessel and a constant angle of insonation. Doppler techniques are prone to overestimation of total blood flow in a vessel as only the highest flow in the center of the vessel is assessed (53, 54). Doppler ultrasound has been used to measure flow during isometric contractions, and during exercise (55-58) however, as the effect of exercise on the diameter of the insonated vessels has not been completely characterized, and as movement may potentially compromise data, the validity of measurements with Doppler may not be entirely valid and accurate (53).

Near-Infrared Spectroscopy (NIRS)

Near-infrared spectroscopy (NIRS) can be used to measure regional oxygen saturation in tissue by analyzing the spectrum of reflected near-infrared light (10, 59, 60). Near-infrared spectroscopy is significantly less expensive, smaller and more portable than larger imaging modalities like MRI and PET. The temporal resolution is sufficient to monitor changes with exercise and, as the device could be affixed to the subject, motion during an exercise challenge could be controlled for (10, 61, 62). However, NIRS is limited to investigation of superficial vessels due to tissue penetration limitations of the light. As well, the accuracy of NIRS measurement may be confounded by contributions from layering arteries and veins (10, 63). While correlation has been found between NIRS and invasive data, NIRS measures relative changes in oxygen saturation and thus cannot provide absolute measurements for oxygen consumption (10, 64).

Positron Emission Tomography (PET)

Positron emission tomography (PET) measures oxygen metabolism by imaging the accumulated inhaled ^{15}O -labeled radiotracers that distribute into the tissue and are converted into ^{15}O -labeled water (10, 65). PET is restrictive in terms of its utility for exercise imaging due to several factors: high radiation dosage, complex, potentially invasive arterial/venous lines for administration of radio-

labeled gases, high associated expenses, comparatively low spatial resolution, and long scan times (66, 67).

Determining the saturation of venous blood returning from a muscle group provides an indirect measurement of the oxygen extraction of that muscle group. As well, while blood flow is commonly measured on the arterial side, the inherent pulsatility of the arterial flow may confound flow measurements. Luckily, the venous blood flow returning from a muscle provides a surrogate measurement of the blood flowing to that muscle group, with less transient pulsatility.

MRI Techniques

Magnetic Resonance Imaging (MRI) is a commonly used imaging technique to investigate anatomy and physiology in health and disease. MRI scanners use a combination of static and time-varying magnetic fields to image water (and other molecules containing hydrogen atoms), with highly controllable soft tissue contrast and the ability to measure a wide array of functional information. Of particular interest in this thesis is the sensitivity of MRI to oxygen saturation and to blood flow, and the ability to image planes with arbitrary orientations.

MRI has previously validated methods to measure flow such as phase contrast and complex-difference imaging (68-70), and previously validated techniques to measure oxygen saturation such as magnetization relaxation based techniques including blood oxygen level dependent (BOLD) and T2-relaxation-under-spin-tagging (TRUST) techniques as well as susceptometry based techniques. None of these techniques have characterized oxygen consumption, and the relative contributions of blood flow and venous oxygen saturation, with an exercise challenge (70).

The techniques to measure flow and oxygen saturation will be discussed below, as well as a brief discussion on exercise in the MRI scanner. Finally, this section will conclude with a brief description on interleaving pulse sequences, a critical characteristic of the new technique fully described in Chapter 2.

Measuring Blood Flow

Phase-Contrast Magnetic Resonance Imaging (PC-MRI) is the current gold standard for measuring blood flow in conduit blood vessels (68, 69). Phase-difference methods are based on the accumulation of phase shift proportional with the velocity of moving hydrogen nuclei (71).

PC-MRI images the magnetized moving spins, thereby obtaining quantitative flow information (72-75). This is achieved by the introduction of a bipolar flow encoding gradient, as shown in Fig. 1.1, after the radio-frequency (RF) excitation pulse and slice selective gradient, to encode the velocity of the moving spins. This velocity is translated into image phase by the flow encoding gradients. The flow gradients can be placed in any physical gradient orientation to achieve flow sensitivity in that direction. Flow gradients can even be applied simultaneously in multiple axes to obtain flow sensitivity in any arbitrary direction.

Phase data obtained from the MRI is influenced by factors like main static magnetic field (B_0) inhomogeneities, radiofrequency coils, and eddy currents. In order to eliminate these unwanted sources of phase, two images are acquired. The first image is obtained with a flow encoding gradient and the second image is acquired flow compensated (without the flow encoding gradient or with a negative flow encoding gradient strength, as shown in Fig. 1.1).

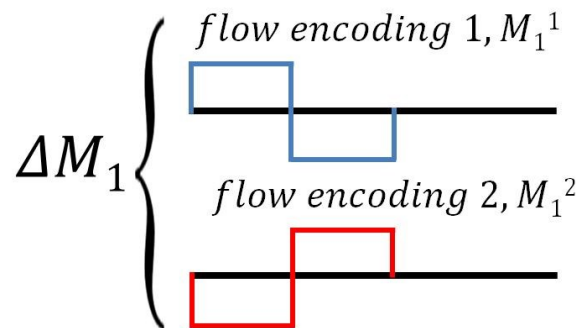


Figure 1.1 – Bipolar gradients with opposite polarities result in different first moments, M_1 . A phase- or complex-difference calculation eliminates the background phase allowing for velocity measurement.

The n^{th} order gradient moment M_n integrals describe the contributions of the magnetic field gradients (76).

$$\varphi(r,TE)=\varphi_0+\gamma r_0 \int_0^{TE} G(t) dt +\gamma v \int_0^{TE} G(t) t dt +\dots \quad \text{Eq. 1.6}$$

Phase φ at an arbitrary point in space, r , and time, TE , is described in Eq. 1.6. φ_0 is the unknown background phase, the second term is the zeroth order gradient moment describing phase encoding from stationary spins. The third term is the first gradient moment, $M_1 = \int_0^{TE} G(t) t dt$. Velocity induced signal phase, for the constant velocity approximation, is proportional to M_1 , ($\varphi_{\text{vel}} = \gamma * v * M_1$) (76).

The phase of these images (ϕ_1 and ϕ_2) are subtracted to remove any non-velocity contributions to phase (including phase encoding from stationary spins, M_0) and velocity is calculated from the resulting phase difference ($\Delta\phi$) image.

$$\phi_1 - \phi_2 = \Delta\phi = \gamma * v * \Delta M_1 \quad \text{Eq. 1.7}$$

The encoding velocity (VENC) is determined by the difference in the first moments of the two interleaved velocity-encoded acquisitions (ΔM_1) and the associated gradient waveforms. VENC is specified by the operator and typically chosen such that $VENC = 1.2 * v_{\text{max}}$, or 1.2 times greater than the maximum expected velocity. If the velocity exceeds VENC then aliasing, or phase wrapping, will occur. VENC represents the velocity value that leads to a flow-induced phase accumulation of $\pm\pi$. Then, from Eq. 1.7 the velocity can be described generally in terms of the VENC and the phase difference of $\Delta\phi$:

$$v = \Delta\phi / (\gamma * \Delta M_1) = \Delta\phi * (VENC / \pi) \quad \text{Eq. 1.8}$$

The encoding velocity (VENC) is defined as a phase difference of π :

$$\text{VENC} = \pi / (\gamma * \Delta M_1) \quad \text{Eq. 1.9}$$

The velocity is then described by the VENC and the phase difference (77):

$$v = \Delta\phi * (\text{VENC} / \pi) \quad \text{Eq. 1.10}$$

Software is used to draw regions around the vessel of interest, as well as around a surrounding stationary reference tissue area, to measure and remove any residual background phase that was not removed by the differential flow-encoding (i.e. phase error most often caused by eddy currents). The area of the vessel (A) is measured by tracing the vessel lumen manually. The number of pixels in the vessel of interest is multiplied by the pixel spacing to obtain the area. Then, the velocity is spatially averaged across the lumen and multiplied by the calculated area (A) to obtain a total quantification of the blood flow (BF) in the vessel of interest.

$$\text{BF} = v * A \quad \text{Eq. 1.11}$$

If flow is not constant over time due to cardiac pulsatility, it is common to use cardiac gating, or real time imaging, to resolve flow over the cardiac cycle, yielding BF values at several cardiac phases. PC-MRI makes no geometric assumptions, and operator variances are minimized with a standardized protocol. PC-MRI provides flexibility in spatial and temporal resolution to suit the application and has access to all directions of flow at any location. PC-MRI has been used to quantify flow during exercise (78).

Complex Difference to Measure Blood Flow

Complex Difference MRI (CD-MRI) is an extension of PC-MRI which can provide qualitative images to visualize flow, or moving spins, and is robust to partial volume effects. In CD-MRI the complex values from two images are subtracted on a pixel-by-pixel basis and the signal from stationary spins is subtracted out (74, 79, 80). Complex difference, as the name suggests, performs the subtraction of the two complex datasets either in k-space or in the image domain.

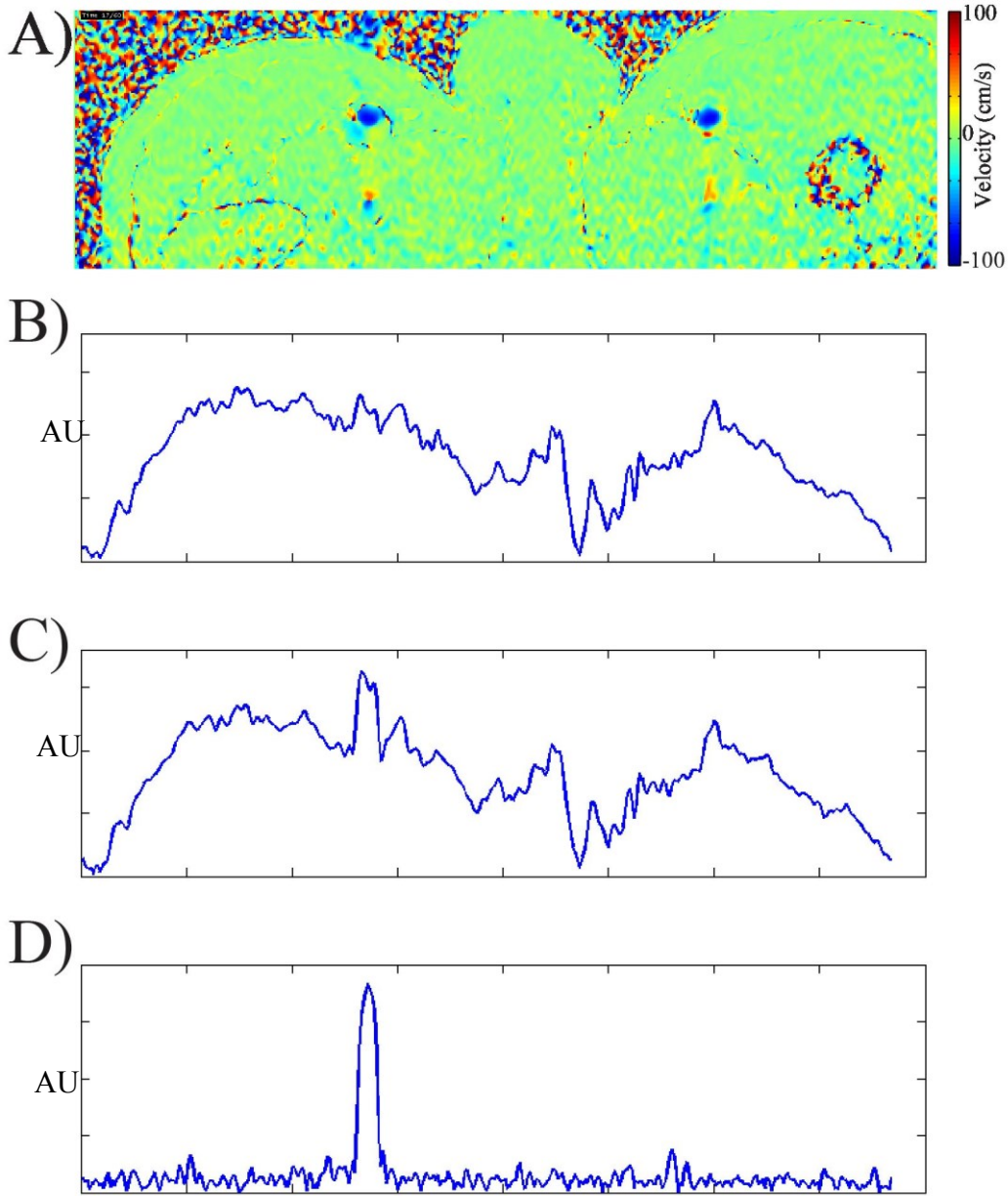


Figure 1.2 – Comparison between phase contrast and complex difference. 1.2A) shows a standard phase contrast acquisition with the highest flow signal measured in the femoral vein. As this is a cardiac gated phase contrast, this image took several seconds to acquire. This data is compared to complex difference acquisition data, where the static tissue is completely subtracted out from the signal by computing the difference between the flow compensated signal projection in 1.2B) with the flow encoded signal project in 1.2C), what remains is only the velocity encoded signal from the moving spins only as seen in 1.2D).

The variant of the CD-MRI imaging method used in this thesis is the line-scan projection CD method. The goal of projection CD-MRI is to speed up traditional PC-MRI techniques, by eliminating the phase-encoding gradients, and

enable real-time velocity imaging, appropriate for quantitatively measuring blood flow in large vessels (81). The values from complex difference flow imaging agree when compared to conventional PC-MRI techniques (81), but the acquisition time is significantly shorter, a comparison is shown in Fig. 1.2. The time savings come from a tradeoff for information on the inhomogeneity of flow in the vessel.

Rapid imaging is necessary for the proposed thesis as the goal is to quantify blood flow in conjunction with dynamic exercise, for which tissue motion and rapidly changing blood velocities preclude conventional PC-MRI techniques (which often have a several second imaging window). The particular details of our complex-difference imaging technique and the practical intricacies of CD-MRI implementation are explored in Chapter 2. The blood flow imaging is only one component of oxygen consumption imaging; the other component is measuring oxygen saturation.

Measuring Oxygen Saturation

Measuring oxygen saturation in venous blood with MRI has been explored in many previous studies with a variety of different techniques; in general these techniques exploit contrast from either relaxation time differences or susceptibility differences.

Relaxation based techniques may noninvasively assess blood oxygenation saturation using MRI. These techniques are based on BOLD (blood oxygen level dependent) contrast imaging. As deoxyhemoglobin concentration increases, magnetization relaxation rate (i.e. T_2 , T_2^* or T_2') decreases.. The relationship between relaxation rates and blood oxygenation has been demonstrated in blood samples, and is a main theory driving the field of functional magnetic resonance imaging, or fMRI (82, 83). An in-vitro calibration curve is required to translate measurements of the relaxation rates into oxygen saturations (10, 84). Previous studies have used relaxation rate measurements to extract the oxygen saturation of the blood (10, 24, 84, 85).

Oxygen saturation has been measured using a T2 relaxation rate from a special multi-echo gradient echo (GRE) / spin echo (SE) sequence (10, 86-93). Static spin dephasing and/or spin diffusion through field inhomogeneity may induce signal loss (10). A multi-echo GRE sequence is typically used to obtain the time constant for transverse magnetization decay from static spin dephasing, or T2* (10, 94-96). T2* decay is more sensitive to oxygen saturation changes than T2 decay as SE signal loss is mainly due to spin diffusion due to field inhomogeneities due to paramagnetic deoxyhemoglobin (10, 96).

A relaxation-based technique has been studied for small vessels (10, 97, 98). T2-Relaxation-Under-Spin-Tagging (TRUST) techniques use a tagging scheme similar to arterial spin labeling for T2 measurements in the vein (99). These techniques are not limited by vessel orientation or the availability of reference tissue for background field measurement. As these relaxation-based techniques require a calibration curve, may be sensitive to pulsatility, and may potentially have longer scan times, susceptibility based techniques may be preferable for imaging the oxygen saturation in venous blood with an exercise challenge (10, 27).

Using Susceptometry to Measure Oxygen Saturation

MRI is sensitive to local perturbations in the main magnetic field (B_0), including those arising from susceptibility effects. The field difference between the inside of the vein of interest and the surrounding tissue (ΔB) is related to the underlying susceptibility difference, and is also dependent on the vessel geometry and orientation. Magnetic susceptibility (χ) is a quantitative measure of the magnetization of a material in response to a magnetic field. Materials may be classified according to susceptibility as paramagnetic ($\chi > 0$), diamagnetic ($\chi < 0$), or ferromagnetic ($\chi \gg 0$). Paramagnetic materials tend to increase the surrounding applied magnetic field, and diamagnetic materials tend to decrease the field.

Hemoglobin (Hgb) has different magnetic properties in its oxygenated and deoxygenated forms, both of which can be detected using MRI (100). In oxyhemoglobin (HbO_2), the iron ion is bound to oxygen with no unpaired electrons,

thus HbO₂ is diamagnetic and creates an induced magnetic field opposite to the applied field. When oxygen dissociates from the ferrous ion it leaves deoxyhemoglobin (dHbO₂) behind. The unpaired electrons of the dHbO₂ molecule make it paramagnetic relative to the surrounding tissue and induce an internal magnetic field in the direction of the applied field (10).

Venous blood rich in dHbO₂ has an increased susceptibility ($\chi > 0$) with respect to the surrounding tissue. This susceptibility difference is an intrinsic contrast agent that causes a shift in the magnetic field, or image phase, relative to surrounding tissues (10). Oxygen saturation of the venous blood (SvO₂) can be related to the susceptibility difference between the venous blood and the surrounding tissue ($\Delta\chi$).

$$\Delta\chi = \Delta\chi_{[do]} * \text{Hct} * (1 - \text{SvO}_2) \quad \text{Eq. 1.12}$$

Hematocrit is the volume percentage of red blood cells in the blood, and the susceptibility difference between fully oxygenated and fully deoxygenated erythrocytes ($\Delta\chi_{[do]}$) has been measured, and validated, at 0.27 ppm (27, 101). Thus, the difference in susceptibility provides an endogenous oxygenation-dependent contrast in-vivo.

An MRI method to quantify oxygen saturation by measuring absolute susceptibility has been developed previously by imaging phase of paramagnetic agents in cylindrical phantoms modeling veins at various oxygenations (102). This technique has been used to measure oxygen saturation from veins in the brain (10, 103, 104), major veins in the neck (27), and major veins in the upper leg (28, 105, 106).

The field changes inside the vessel can be estimated using axial imaging slices orthogonal to the main magnetic field (B_0) direction, and restricting analysis to through-plane vessels parallel or near parallel to B_0 , with a diameter much smaller than the length of the vessel (24, 43, 92). These vessels are approximated as infinite cylinders, for which the inversion from field shift ΔB to susceptibility

shift $\Delta\chi$ is straightforward. This approximation holds well even if the vessel is slightly tilted ($<30^\circ$) with respect to the main magnetic field (43, 107).

The difference in phase between two images is directly related to the incremental field ΔB . The blood vessel can be modeled as a long paramagnetic cylinder, and then the incremental field inside the cylinder ΔB is defined below.

$$\Delta B = 1/6 * \Delta\chi * (3 * \cos^2\theta - 1) * B_0 \quad \text{Eq. 1.13}$$

The susceptibility difference is calculated from a phase difference image obtained by taking the complex difference of two images separated by echo time (TE). By acquiring gradient echo images at multiple TEs and measuring phase differences between the vessel and background tissue, the local field shift can be determined. Phase evolves with time as described below, where gamma, $\gamma = 267.513$ rad/sT, is the gyromagnetic ratio for a ^1H proton (108).

$$\Delta\phi = \gamma * \Delta B * \Delta TE \quad \text{Eq. 1.14}$$

Echo time should be short enough to avoid unwanted phase wrapping (27). By combining Equations 1.12, 1.13, and 1.14, the venous oxygen saturation (SvO_2) is related to the phase shift ($\Delta\phi / \Delta TE$):

$$\text{SvO}_2(\%) = 100 * \left\{ 1 - \frac{2 * |\Delta\phi / \Delta TE|}{\gamma * \chi_{\text{do}} * \text{Hct} * B_0 * (\cos^2\theta - 1/3)} \right\} \quad \text{Eq. 1.15}$$

In Equation 1.13, the venous oxygen saturation can be calculated from the measured phase shift. The hematocrit value is assumed to be $\text{Hct} = 0.42$ (109) for a healthy young male, the gyromagnetic ratio and main magnetic field strength are known, the susceptibility difference between oxygenated and deoxygenated blood has been previously calculated and validated (101) and the angle between the vessel can be measured from a stack of images along the vein (107).

With the blood flow and venous oxygen saturation calculated above and a healthy normal assumed arterial saturation ($SaO_2 = 98\%$), oxygen consumption can be calculated from using Eq. 1.5 (47). Hemoglobin can be measured, or assumed to be 146 mmol/L and the carrying capacity of oxygen can be calculated from this value for Hgb ($Ca = 1.34 \text{ ml O}_2/\text{g of Hgb}$). Thus all that is needed to estimate local muscle tissue oxygen consumption is a measure of blood flow (Q) to the muscle and venous oxygen saturation (SvO_2) in the blood draining from the muscle.

Flow and oxygen saturation should be measured simultaneously and fast enough to characterize the rapid hemodynamic changes that accompany exercise and exercise cessation. Thus, the complex difference flow imaging technique must be combined with the susceptibility oxygen saturation imaging technique, to create an interleaved sequence.

Interleaved Flow and Oxygen Saturation Imaging

Simultaneous measurement of skeletal muscle blood flow and oxygen saturation allows characterization of the oxygen metabolism of the working muscle, including detailed insight into the components of oxygen consumption. Independent imaging of the factors could introduce potential confounders which are difficult to control for. This simultaneous imaging is made possible by interleaving sequences for flow and oxygen saturation measurement.

There is some published research on interleaving a phase contrast MRI sequence with a susceptibility sequence for simultaneous mapping of blood flow and oxygenation at rest and during post-occlusive reactive hyperemia (28). By using phase projections, which are explained in detail in Chapter 2, interleaved imaging can be accelerated. Jain et al. accomplished a temporal resolution of 2.5s, with a similar phase-contrast MRI-based approach, by utilizing phase projections (110). Exercise in the MRI is a difficult challenge with many applications. Characterization of maximal oxygen consumption and recovery from exercise is made possible by imaging before and immediately post-exercise.

Exercise in the MRI

Exercise challenges provide information on the stressed state, and recovery, of tissue perfusion and oxygen consumption abnormalities otherwise hidden at rest (37). Exercise in an MRI requires special equipment that is MRI compatible. The device must allow for exercise in the narrow bore of the MRI where leg movement is restricted and must allow for alignment with the magnetic isocenter. Several design factors must be considered for in-magnet exercise devices, such as robustness, minimal power loss due to friction, adjustability based on height and leg length, accurate quantification of a variable workload, safety, security, and comfort.

Several attempts have been made to facilitate exercise in the MRI room (111, 112) prior to imaging alignment, as well as directly in the MRI bore (41, 42, 113-115). On-bed exercise is preferable for a variety of reasons, including the following: the hemodynamic deviations with exercise will retreat to baseline quite suddenly following the cessation of the exercise challenge (37, 116) and the patient does not need to be repositioned after the exercise challenge.

The physiological goal of the major study comprising this thesis is to simultaneously measure the components of oxygen consumption (blood flow and oxygen extraction) in an isolated working muscle while minimizing the potentially limiting factor of cardiac output, or delivery of O₂. Thus, the muscle group should be a single well-defined functional group, exercisable in isolation, with direct blood flow to and from the muscle group. The quadriceps muscle, specifically exercised with a dynamic knee-extension exercise, is an ideal candidate for these requirements. We designed an exercise device to meet the necessary criteria for MRI-compatible knee-extension exercise, as no device was commercially available.

Scope of Thesis

In this thesis a new imaging technique to simultaneously measure blood flow, oxygen saturation, and calculate and characterize oxygen metabolism in an exercising muscle mass is proposed. There are three chapters in this thesis: Chapter

1 provides a motivation for measuring these physiological values as well as the background knowledge associated with the thesis. Furthermore, previous studies with similar interests in measuring these physiological values, as well as their limitations, are discussed. In Chapter 2, the main body of the thesis, the new technique is presented which uses a new interleaved MRI technique to simultaneously measure skeletal muscle oxygen consumption and venous blood flow with an exercise challenge. Accompanying the study in chapter 2 is a comparison of the results of the new technique with existing measures for blood flow and oxygen metabolism with exercise. Chapter 3 discusses the results of the study presented in Chapter 2 in the larger context of the intersection of exercise physiology and biomedical imaging; as well, limitations of the study and future directions of the technique and the field of research are discussed.

We endeavored to design and build an MRI compatible knee-extension ergometer with a variable, quantifiable workload. In parallel with the development of the exercise ergometer, a novel MRI imaging technique interleaving flow-sensitive complex difference acquisitions with oxygenation sensitive multi-gradient echo acquisitions was tested and developed. Following testing of the exercise device and the imaging sequence, a pilot study was designed and undertaken to test the feasibility and reproducibility of the simultaneous measurement of femoral vein blood flow and venous blood oxygenation. From this simultaneously acquired blood flow and oxygen extraction, the metabolic rate of oxygen consumption in skeletal muscle in healthy adult volunteers was measured at rest and immediately post-knee extension exercise. In addition, the oxygen off-kinetics was obtained by fitting the muscle VO_2 relaxation data with a mono-exponential function. These measured parameters are compared between two trials to assess the reproducibility of the technique. This study, with additional details on methods, is presented in Chapter 2 of this thesis. Direct comparisons between our study and other studies are difficult due to variances in exercise protocols and measured parameters (29, 115, 117).

The research presented in this thesis outlines the background, development, and testing of a novel MRI-based muscle susceptometry approach for simultaneous measurement of oxygen extraction, blood flow, and oxygen consumption immediately post single-leg knee-extension exercise within the MRI magnet bore. By endeavoring to measure and characterize these physiological parameters, we can improve the testing and treatment progressions for pathologies that limit exercise capacity such as heart failure, diabetes, and cancer.

Chapter 1 References

- [1] Levy WC, Maichel Ba, Steele NP, Leclerc KM, Stratton JR. Biomechanical efficiency is decreased in heart failure during low-level steady state and maximal ramp exercise. *European journal of heart failure* 2004;6(7):917-26.
- [2] Witte KK, Levy WC, Lindsay Ka, Clark AL. Biomechanical efficiency is impaired in patients with chronic heart failure. *European journal of heart failure* 2007;9(8):834-8.
- [3] Piña IL, Apstein CS, Balady GJ, Belardinelli R, Chaitman BR, Duscha BD, Fletcher BJ, Fleg JL, Myers JN, Sullivan MJ. Exercise and heart failure a statement from the american heart association committee on exercise, rehabilitation, and prevention. *Circulation* 2003;107(8):1210-25.
- [4] Balady GJ, Arena R, Sietsema K, Myers J, Coke L, Fletcher GF, Forman D, Franklin B, Guazzi M, Gulati M. Clinician's guide to cardiopulmonary exercise testing in adults a scientific statement from the american heart association. *Circulation* 2010;122(2):191-225.
- [5] Coronel R, De Groot J, Van Lieshout J. Defining heart failure. *Cardiovascular research* 2001;50(3):419-22.
- [6] Bui AL, Horwich TB, Fonarow GC. Epidemiology and risk profile of heart failure. *Nat Rev Cardiol* 2011;8(1):30-41.
- [7] Moe GW, Ezekowitz JA, O'Meara E, Howlett JG, Fremes SE, Al-Hesayen A, Heckman GA, Ducharme A, Estrella-Holder E, Grzeslo A. The 2013 canadian cardiovascular society heart failure management guidelines update: Focus on rehabilitation and exercise and surgical coronary revascularization. *Canadian Journal of Cardiology* 2014;30(3):249-63.
- [8] Ross H, Howlett J, Arnold JMO, Liu P, O'Neill B, Brophy J, Simpson C, Sholdice M, Knudtson M, Ross D. Treating the right patient at the right time: Access to heart failure care. *Canadian journal of Cardiology* 2006;22(9):749-54.
- [9] Arnold JMO, Liu P, Demers C, Dorian P, Giannetti N, Haddad H, Heckman GA, Howlett JG, Ignaszewski A, Johnstone DE. Canadian cardiovascular society consensus conference recommendations on heart failure 2006: Diagnosis and management. *Canadian Journal of Cardiology* 2006;22(1):23-45.
- [10] Tang, J. Quantification of Oxygen Saturation of Venous Vessels Using Susceptibility Mapping. McMaster University; 2012.
- [11] Billett, HH. Hemoglobin and Hematocrit. In: Walker, HK, Hall, WD, Hurst, JW, editors. *Clinical Methods: The History, Physical, and Laboratory*

Examinations. Boston: Butterworth Publishers, a division of Reed Publishing; 1990.

- [12] Dominguez de Villota ED, Ruiz Carmona MT, Rubio JJ, de Andres S. Equality of the in vivo and in vitro oxygen-binding capacity of haemoglobin in patients with severe respiratory disease. *British journal of anaesthesia* 1981;53(12):1325-8.
- [13] Weber KT, Kinasewitz GT, Janicki JS, Fishman AP. Oxygen utilization and ventilation during exercise in patients with chronic cardiac failure. *Circulation* 1982;65(6):1213-23.
- [14] Gallagher P, Farrell A. 6 hematocrit and blood oxygen-carrying capacity. *Fish physiology* 1998;17:185-227.
- [15] Bassett D, Howley ET. Limiting factors for maximum oxygen uptake and determinants of endurance performance. *Medicine and science in sports and exercise* 2000;32(1):70-84.
- [16] Rowell LB, Taylor HL, Wang Y, Carlson WS. Saturation of arterial blood with oxygen during maximal exercise. *Journal of Applied Physiology* 1964;19(2):284-6.
- [17] Richardson RS, Knight DR, Poole DC, Kurdak SS, Hogan MC, Grassi B, Wagner PD. Determinants of maximal exercise VO₂ during single leg knee-extensor exercise in humans. *American Journal of Physiology-Heart and Circulatory Physiology* 1995;37(4):H1453.
- [18] Richardson R, Frank L, Haseler L. Dynamic knee-extensor and cycle exercise: Functional MRI of muscular activity. *International journal of sports medicine* 1998;19(03):182-7.
- [19] Arthur C. Guyton, JE. *Textbook of Medical Physics*. Philadelphia: Elsevier Inc.; 2006.
- [20] Ekblom B, Astrand PO, Saltin B, Stenberg J, Wallstrom B. Effect of training on circulatory response to exercise. *J Appl Physiol* 1968;24:518-528.
- [21] Williams JH, Powers SK, Stuart MK. Hemoglobin desaturation in highly trained athletes during heavy exercise. *Medicine and science in sports and exercise* 1986;18(2):168-73.
- [22] Pittman, RN. Chapter 7 Oxygen transport in normal and pathological situations: defects and compensations. In: *Regulation of Tissue Oxygenation* 2011.

- [23] Blomstrand E, Rådegran G, Saltin B. Maximum rate of oxygen uptake by human skeletal muscle in relation to maximal activities of enzymes in the krebs cycle. *The Journal of Physiology* 1997;501(Pt 2):455-60.
- [24] van Zijl PC, Eleff SM, Ulatowski JA, Oja JM, Ulug AM, Traystman RJ, Kauppinen RA. Quantitative assessment of blood flow, blood volume and blood oxygenation effects in functional magnetic resonance imaging. *Nature medicine* 1998;4(2):159-67.
- [25] Macmillan CS, Andrews PJ. Cerebrovenous oxygen saturation monitoring: Practical considerations and clinical relevance. *Intensive care medicine* 2000;26(8):1028-36.
- [26] West, JB. *Pulmonary physiology and pathophysiology: an integrated, case-based approach*. Lippincott Williams & Wilkins; 2007.
- [27] Jain V, Langham MC, Wehrli FW. MRI estimation of global brain oxygen consumption rate. *Journal of Cerebral Blood Flow & Metabolism* 2010;30(9):1598-607.
- [28] Langham MC, Wehrli FW. Simultaneous mapping of temporally-resolved blood flow velocity and oxygenation in femoral artery and vein during reactive hyperemia. *Journal of Cardiovascular Magnetic Resonance* 2011;13:66.
- [29] Andersen P, Saltin B. Maximal perfusion of skeletal muscle in man. *The Journal of Physiology* 1985(1985):233-49.
- [30] Armstrong WF, Zoghbi WA. Stress echocardiography: Current methodology and clinical applications. *Journal of the American College of Cardiology* 2005;45(11):1739-47.
- [31] Myers J, Gullestad L. The role of exercise testing and gas-exchange measurement in the prognostic assessment of patients with heart failure. *Current opinion in cardiology* 1998;13(3):145-55.
- [32] Myers J. Applications of cardiopulmonary exercise testing in the management of cardiovascular and pulmonary disease. *International journal of sports medicine* 2005;26(S 1):S49-55.
- [33] Ribeiro JP, Stein R, Chiappa GR. Beyond peak oxygen uptake: New prognostic markers from gas exchange exercise tests in chronic heart failure. *Journal of Cardiopulmonary Rehabilitation and Prevention* 2006;26(2):63-71.
- [34] Sullivan MJ, Knight J, Higginbotham M, Cobb F. Relation between central and peripheral hemodynamics during exercise in patients with chronic heart

- failure. muscle blood flow is reduced with maintenance of arterial perfusion pressure. *Circulation* 1989;80(4):769-81.
- [35] Myers J, Froelicher VF. Hemodynamic determinants of exercise capacity in chronic heart failure. *Annals of internal medicine* 1991;115(5):377-86.
- [36] Saltin AS. Cardiac output during submaximal and maximal work. 1964.
- [37] Saltin B. Hemodynamic adaptations to exercise. *The American Journal of Cardiology* 1985;55(10):D42-7.
- [38] Braden D, Carroll J. Normative cardiovascular responses to exercise in children. *Pediatric cardiology* 1999;20(1):4-10.
- [39] Hill AV, Lupton H. Muscular exercise, lactic acid, and the supply and utilization of oxygen. *Q J Med* 1923;16(62):135-71.
- [40] Casey DP, Joyner MJ. Skeletal muscle blood flow responses to hypoperfusion at rest and during rhythmic exercise in humans. *Journal of applied physiology* 2009;107(2):429-37.
- [41] Weber TF, von Tengg-Kobligk H, Kopp-Schneider A, Ley-Zaporozhan J, Kauczor H, Ley S. High-resolution phase-contrast MRI of aortic and pulmonary blood flow during rest and physical exercise using a MRI compatible bicycle ergometer. *European journal of radiology* 2011;80(1):103-8.
- [42] Cheng CP, Herfkens RJ, Taylor CA, Feinstein JA. Proximal pulmonary artery blood flow characteristics in healthy subjects measured in an upright posture using MRI: The effects of exercise and age. *Journal of Magnetic Resonance Imaging* 2005;21(6):752-8.
- [43] Langham MC, Magland JF, Epstein CL, Floyd TF, Wehrli FW. Accuracy and precision of MR blood oximetry based on the long paramagnetic cylinder approximation of large vessels. *Magnetic Resonance in Medicine* 2009;62(2):333-40.
- [44] Boushel R, Langberg H, Green S, Skovgaard D, Bülow J, Kjær M. Blood flow and oxygenation in peritendinous tissue and calf muscle during dynamic exercise in humans. *The Journal of physiology* 2000;524(1):305-13.
- [45] Kety SS. Measurement of regional circulation by the local clearance of radioactive sodium. *American heart journal* 1949;38(3):321-8.
- [46] Kety SS, Schmidt CF. The effects of altered arterial tensions of carbon dioxide and oxygen on cerebral blood flow and cerebral oxygen consumption of normal young men. *Journal of Clinical Investigation* 1948;27(4):484.

- [47] Kety SS, Schmidt CF. The nitrous oxide method for the quantitative determination of cerebral blood flow in man; theory, procedure and normal values. *Journal of Clinical Investigation* 1948;27(4):476-83.
- [48] Mayberg T, Lam A. Jugular bulb oximetry for the monitoring of cerebral blood flow and metabolism. *Neurosurgery clinics of North America* 1996;7(4):755-65.
- [49] Andersen P, Adams RP, Sjogaard G, Thorboe A, Saltin B. Dynamic knee extension as model for study of isolated exercising muscle in humans. *Journal of applied physiology* 1985;59(5):1647-53.
- [50] Coplin WM, O'Keefe GE, Grady MS, Grant GA, March KS, Winn HR, Lam AM. Thrombotic, infectious, and procedural complications of the jugular bulb catheter in the intensive care unit. *Neurosurgery* 1997;41(1):101-9.
- [51] Gill RW. Pulsed doppler with B-mode imaging for quantitative blood flow measurement. *Ultrasound in medicine & biology* 1979;5(3):223-35.
- [52] Hoskins P. Measurement of arterial blood flow by doppler ultrasound. *Clinical physics and physiological measurement* 1990;11(1):1.
- [53] Gill RW. Measurement of blood flow by ultrasound: Accuracy and sources of error. *Ultrasound in medicine & biology* 1985;11(4):625-41.
- [54] Eicke BM, Kremkau FW, Hinson H, Tegeler CH. Peak velocity overestimation and linear-array spectral doppler. *Journal of neuroimaging*. 1995;5(2):115-21.
- [55] Wesche J. The time course and magnitude of blood flow changes in the human quadriceps muscles following isometric contraction. *The Journal of physiology* 1986;377(1):445-62.
- [56] Walløe L, Wesche J. Time course and magnitude of blood flow changes in the human quadriceps muscles during and following rhythmic exercise. *The Journal of physiology* 1988;405(1):257-73.
- [57] Shoemaker J, Phillips S, Green H, Hughson R. Faster femoral artery blood velocity kinetics at the onset of exercise following short-term training. *Cardiovascular research* 1996;31(2):278-86.
- [58] Rådegran G. Ultrasound doppler estimates of femoral artery blood flow during dynamic knee extensor exercise in humans. *Journal of Applied Physiology* 1997;83(4):1383-8.

- [59] Daubeney PE, Pilkington SN, Janke E, Charlton GA, Smith DC, Webber SA. Cerebral oxygenation measured by near-infrared spectroscopy: Comparison with jugular bulb oximetry. *The Annals of thoracic surgery* 1996;61(3):930-4.
- [60] Van Beekvelt MC, Colier WN, Wevers RA, Van Engelen BG. Performance of near-infrared spectroscopy in measuring local O₂ consumption and blood flow in skeletal muscle. *Journal of Applied Physiology* 2001;90(2):511-9.
- [61] Jobsis FF. Noninvasive, infrared monitoring of cerebral and myocardial oxygen sufficiency and circulatory parameters. *Science (New York, N Y)* 1977;198(4323):1264-7.
- [62] Wahr JA, Tremper KK, Samra S, Delpy DT. Near-infrared spectroscopy: Theory and applications. *Journal of cardiothoracic and vascular anesthesia* 1996;10(3):406-18.
- [63] Nagdyman N, Fleck T, Schubert S, Ewert P, Peters B, Lange PE, Abdul-Khaliq H. Comparison between cerebral tissue oxygenation index measured by near-infrared spectroscopy and venous jugular bulb saturation in children. *Intensive care medicine* 2005;31(6):846-50.
- [64] Tortoriello TA, Stayer SA, Mott AR, Dean McKenzie E, Fraser CD, Andropoulos DB, Chang AC. A noninvasive estimation of mixed venous oxygen saturation using near-infrared spectroscopy by cerebral oximetry in pediatric cardiac surgery patients. *Pediatric Anesthesia* 2005;15(6):495-503.
- [65] Ito H, Ibaraki M, Kanno I, Fukuda H, Miura S. Changes in cerebral blood flow and cerebral oxygen metabolism during neural activation measured by positron emission tomography: Comparison with blood oxygenation level-dependent contrast measured by functional magnetic resonance imaging. *Journal of Cerebral Blood Flow & Metabolism* 2005;25(3):371-7.
- [66] Frackowiak RS, Lenzi GL, Jones T, Heather JD. Quantitative measurement of regional cerebral blood flow and oxygen metabolism in man using ¹⁵O and positron emission tomography: Theory, procedure, and normal values. *Journal of computer assisted tomography* 1980;4(6):727-36.
- [67] Mintun MA, Raichle ME, Martin WR, Herscovitch P. Brain oxygen utilization measured with O-15 radiotracers and positron emission tomography. *Journal of nuclear medicine : official publication, Society of Nuclear Medicine* 1984;25(2):177-87.
- [68] Ho SSY, Chan YL, Yeung DKW, Metreweli C. Blood flow volume quantification of cerebral ischemia: Comparison of three noninvasive imaging techniques of carotid and vertebral arteries. *American Journal of Roentgenology* 2002;178(3):551-6.

- [69] Spilt A, Box F, van der Geest RJ, Reiber JH, Kunz P, Kamper AM, Blauw GJ, van Buchem MA. Reproducibility of total cerebral blood flow measurements using phase contrast magnetic resonance imaging. *Journal of Magnetic Resonance Imaging* 2002;16(1):1-5.
- [70] Barhoum S, Rodgers ZB, Langham M, Magland JF, Li C, Wehrli FW. Comparison of MRI methods for measuring whole-brain venous oxygen saturation. *Magnetic Resonance in Medicine* 2014.
- [71] Hundley WG, Li HF, Hillis LD, Meshack BM, Lange RA, Willard JE, Landau C, Peshock RM. Quantitation of cardiac output with velocity-encoded, phase-difference magnetic resonance imaging. *The American journal of cardiology* 1995;75(17):1250-5.
- [72] Moran PR. A flow velocity zeugmatographic interlace for NMR imaging in humans. *Magnetic resonance imaging* 1982;1(4):197-203.
- [73] Axel L. Blood flow effects in magnetic resonance imaging. *American journal of roentgenology* 1984;143(6):1157-66.
- [74] Bryant D, Payne J, Firmin D, Longmore D. Measurement of flow with NMR imaging using a gradient pulse and phase difference technique. *Journal of computer assisted tomography* 1984;8(4):588-93.
- [75] Moran P, Saloner D, Tsui B. NMR velocity-selective excitation composites for flow and motion imaging and suppression of static tissue signal. *Medical Imaging, IEEE Transactions on* 1987;6(2):141-7.
- [76] Markl, M. *Velocity Encoding and Flow Imaging*. 2005.
- [77] Langham MC, Jain V, Magland JF, Wehrli FW. Time-resolved absolute velocity quantification with projections. *Magnetic resonance in medicine*. 2010;64(6):1599-606.
- [78] Gatehouse PD, Keegan J, Crowe LA, Masood S, Mohiaddin RH, Kreitner K, Firmin DN. Applications of phase-contrast flow and velocity imaging in cardiovascular MRI. *European radiology* 2005;15(10):2172-84.
- [79] O'Donnell M. NMR blood flow imaging using multiecho, phase contrast sequences. *Medical physics* 1985;12(1):59-64.
- [80] Dumoulin C, Souza S, Walker M, Wagle W. Three-dimensional phase contrast angiography. *Magnetic Resonance in Medicine* 1989;9(1):139-49.
- [81] Thompson RB, McVeigh ER. Real-time volumetric flow measurements with complex-difference MRI. *Magnetic Resonance in Medicine* 2003;50(6):1248-55.

- [82] Thulborn KR, Waterton JC, Matthews PM, Radda GK. Oxygenation dependence of the transverse relaxation time of water protons in whole blood at high field. *Biochimica et biophysica acta* 1982;714(2):265-70.
- [83] Gomori JM, Grossman RI, Yu-IP C, Asakura T. NMR relaxation times of blood: Dependence on field strength, oxidation state, and cell integrity. *Journal of computer assisted tomography* 1987;11(4):684-90.
- [84] Wright GA, Hu BS, Macovski A. Estimating oxygen saturation of blood in vivo with MR imaging at 1.5 T. *Magnetic Resonance Imaging* 1991:275-83.
- [85] Oja JM, Gillen JS, Kauppinen RA, Kraut M, van Zijl PC. Determination of oxygen extraction ratios by magnetic resonance imaging. *Journal of Cerebral Blood Flow & Metabolism* 1999;19(12):1289-95.
- [86] Yablonskiy DA, Haacke EM. Theory of NMR signal behavior in magnetically inhomogeneous tissues: The static dephasing regime. *Magnetic Resonance in Medicine* 1994;32(6):749-63.
- [87] He X, Yablonskiy DA. Quantitative BOLD: Mapping of human cerebral deoxygenated blood volume and oxygen extraction fraction: Default state. *Magnetic Resonance in Medicine* 2007;57(1):115-26.
- [88] He X, Zhu M, Yablonskiy DA. Validation of oxygen extraction fraction measurement by qBOLD technique. *Magnetic Resonance in Medicine* 2008;60(4):882-8.
- [89] An H, Lin W. Quantitative measurements of cerebral blood oxygen saturation using magnetic resonance imaging. *Journal of Cerebral Blood Flow & Metabolism* 2000;20(8):1225-36.
- [90] An H, Lin W, Celik A, Lee YZ. Quantitative measurements of cerebral metabolic rate of oxygen utilization using MRI: A volunteer study. *NMR in Biomedicine* 2001;14(7-8):441-7.
- [91] An H, Lin W. Cerebral oxygen extraction fraction and cerebral venous blood volume measurements using MRI: Effects of magnetic field variation. *Magnetic resonance in medicine* 2002;47(5):958-66.
- [92] Yablonskiy DA, Haacke EM. An MRI method for measuring T2 in the presence of static and RF magnetic field inhomogeneities. *Magnetic resonance in medicine* 1997;37(6):872-6.
- [93] Yablonskiy DA, Reinus WR, Stark H, Haacke EM. Quantitation of T2' anisotropic effects on magnetic resonance bone mineral density measurement. *Magnetic resonance in medicine* 1997;37(2):214-21.

- [94] Chien D, Levin DL, Anderson CM. MR gradient echo imaging of intravascular blood oxygenation: T2* determination in the presence of flow. *Magnetic resonance in medicine* 1994;32(4):540-5.
- [95] Li D, Waight DJ, Wang Y. In vivo correlation between blood T2 and oxygen saturation. *Journal of Magnetic Resonance Imaging* 1998;8(6):1236-9.
- [96] Li D, Wang Y, Waight DJ. Blood oxygen saturation assessment in vivo using T2* estimation. *Magnetic resonance in medicine* 1998;39(5):685-90.
- [97] Sedlacik J, Rauscher A, Reichenbach JR. Quantification of modulated blood oxygenation levels in single cerebral veins by investigating their MR signal decay. *Zeitschrift für Medizinische Physik* 2009;19(1):48-57.
- [98] Sedlacik J, Reichenbach JR. Validation of quantitative estimation of tissue oxygen extraction fraction and deoxygenated blood volume fraction in phantom and in vivo experiments by using MRI. *Magnetic Resonance in Medicine* 2010;63(4):910-21.
- [99] Lu H, Ge Y. Quantitative evaluation of oxygenation in venous vessels using T2-relaxation-under-spin-tagging MRI. *Magnetic resonance in medicine* 2008;60(2):357-63.
- [100] Ogawa S, Lee TM, Kay AR, Tank DW. Brain magnetic resonance imaging with contrast dependent on blood oxygenation. *Proceedings of the National Academy of Sciences of the United States of America* 1990;87(24):9868-72.
- [101] Jain V, Abdulmalik O, Propert KJ, Wehrli FW. Investigating the magnetic susceptibility properties of fresh human blood for noninvasive oxygen saturation quantification. *Magnetic resonance in medicine* 2012;68(3):863-7.
- [102] Weisskoff RM, Kühne S. MRI susceptometry: Image-based measurement of absolute susceptibility of MR contrast agents and human blood. *Magnetic Resonance in Medicine* 1992;24(2):375-83.
- [103] Haacke EM, Lai S, Reichenbach JR, Kuppusamy K, Hoogenraad FG, Takeichi H, Lin W. In vivo measurement of blood oxygen saturation using magnetic resonance imaging: A direct validation of the blood oxygen level-dependent concept in functional brain imaging. *Human brain mapping* 1997;5(5):341-6.
- [104] Liu Y, Pu Y, Fox PT, Gao J. Quantification of dynamic changes in cerebral venous oxygenation with MR phase imaging at 1.9 T. *Magnetic resonance in medicine* 1999;41(2):407-11.

- [105] Langham MC, Magland JF, Floyd TF, Wehrli FW. Retrospective correction for induced magnetic field inhomogeneity in measurements of large-vessel hemoglobin oxygen saturation by MR susceptometry. *Magnetic resonance in medicine* 2009;61(3):626-33.
- [106] Langham MC, Floyd TF, Mohler ER, Magland JF, Wehrli FW. Evaluation of cuff-induced ischemia in the lower extremity by magnetic resonance oximetry. *Journal of the American College of Cardiology* 2010;55(6):598-606.
- [107] Li C, Langham MC, Epstein CL, Magland JF, Wu J, Gee J, Wehrli FW. Accuracy of the cylinder approximation for susceptometric measurement of intravascular oxygen saturation. *Magnetic resonance in medicine* 2012;67(3):808-13.
- [108] Levitt, MH. *Spin dynamics: basic principles of NMR spectroscopy*. Wiley; 2001.
- [109] Guyton AC, Hall J. *Textbook of medical physiology*. WB Saunder's Co., Philadelphia 2000;10th Edition.
- [110] Jain V, Magland J, Langham M, Wehrli FW. High temporal resolution in vivo blood oximetry via projection-based T2 measurement. *Magnetic Resonance in Medicine* 2013;70(3):785-90.
- [111] Foster EL, Arnold JW, Jekic M, Bender JA, Balasubramanian V, Thavendiranathan P, Dickerson JA, Raman SV, Simonetti OP. MR-compatible treadmill for exercise stress cardiac magnetic resonance imaging. *Magnetic Resonance in Medicine* 2012;67(3):880-9.
- [112] Thavendiranathan P, Dickerson J, Scandling D, Balasubramanian V, Hall N, Foster E, Arnold JW, Pennell M, Simonetti OP, Raman SV. Myocardial function and perfusion assessment with exercise stress cardiovascular magnetic resonance using an MRI-compatible treadmill in patients referred for stress SPECT. *Journal of Cardiovascular Magnetic Resonance* 2012;14(Suppl 1):P1.
- [113] Raymer GH, Allman BL, Rice CL, Marsh GD, Thompson RT. Characteristics of a MR-compatible ankle exercise ergometer for a 3.0 T head-only MR scanner. *Medical engineering & physics* 2006;28(5):489-94.
- [114] Ghomi RH, Bredella MA, Thomas BJ, Miller KK, Torriani M. Modular MR-compatible lower leg exercise device for whole-body scanners. *Skeletal radiology* 2011;40(10):1349-54.
- [115] Gusso S, Salvador C, Hofman P, Cutfield W, Baldi JC, Taberner A, Nielsen P. Design and testing of an MRI-compatible cycle ergometer for non-

invasive cardiac assessments during exercise. *Biomedical engineering online* 2012;11:13.

[116] Rossiter H, Ward S, Kowalchuk J, Howe F, Griffiths J, Whipp B. Effects of prior exercise on oxygen uptake and phosphocreatine kinetics during high-intensity knee-extension exercise in humans. *The Journal of Physiology* 2001;537(1):291-303.

[117] Roest A, Lamb H, Van Der Wall E, Vliegen H, Van Den Aardweg J, Kunz P, De Roos A, Helbing W. Cardiovascular response to physical exercise in adult patients after atrial correction for transposition of the great arteries assessed with magnetic resonance imaging. *Heart* 2004;90(6):678-84.

Chapter 2: Feasibility and Reproducibility of Measurement of Skeletal Muscle Blood Flow, Oxygen Extraction and VO₂ with Dynamic Exercise Using MRI¹

Introduction

Maximal pulmonary oxygen uptake (Pulmonary VO_{2max}) is the gold standard measure of aerobic power (1). In accordance with the Fick principle, VO₂ is equal to the product of cardiac output and arterial-venous oxygen content difference (A-VO₂ diff) (2) therefore abnormalities in convective or diffusive O₂ transport and/or impaired oxygen utilization may limit pulmonary VO_{2max}. Decreased pulmonary VO₂ during peak endurance exercise incorporating a large muscle mass (i.e. treadmill or cycling) is a cardinal feature in clinical populations including heart failure patients with preserved or reduced ejection fraction (3, 4). A limitation of pulmonary VO₂ during whole body exercise is that it integrates all factors that determine oxygen consumption, including cardiac output, vascular function, and oxygen extraction in all exercising muscles. Thus, this test cannot identify or distinguish blood flow and oxygen extraction limitations of the exercising muscle in isolation. Conflicting studies regarding either the alteration (5, 6), or lack of alteration (7, 8), of mitochondrial coupling and/or muscular efficiency in heart failure during exercise underlies the need for muscle-specific tests of oxygen consumption that can distinguish the components of blood flow and oxygen extraction to muscle VO₂ with exercise challenges, independently of cardiac output. Previously, isolated muscle VO₂ during dynamic exercise has been measured using femoral and arterial catheters to determine O₂ extraction, combined with a

¹ A version of Chapter 2 of this thesis has been submitted for publication for consideration to Magnetic Resonance in Medicine (MRM) as Mathewson KW, Haykowsky MJ, Thompson RB. Feasibility and Reproducibility of Measurement of Whole Muscle Blood Flow, Oxygen Extraction and VO₂ with Dynamic Exercise Using MRI. (submitted August 2014).

simultaneous measure of muscle blood flow (invasive flow probe, or non-invasive ultrasound) which limits its use to healthy subjects in a clinical setting (9-11).

Non-invasive imaging of muscle VO_2 has been reported with positron emission tomography (PET), but this method is limited by reliance on contrast agents and exposure to ionizing radiation (12, 13). Alternatively, MRI is well suited for the assessment of oxygen delivery and consumption due to its intrinsic sensitivity to both the concentration of deoxyhemoglobin and to blood flow without the requirement for contrast agents or ionizing radiation, in combination with excellent soft tissue contrast. Many studies have used the sensitivity of transverse relaxation rates, R_2 and R_2^* , to changes in deoxyhemoglobin concentration to detect changes in oxygen saturation in blood (14-18) and muscle tissue (19-21). Specifically relevant to the goals of the current study, Elder et al (20) and later Zheng et al (19) used MR methods to measure relative oxygen saturation and perfusion in the calf muscle with isometric contraction. While these studies have illustrated direct imaging of flow and oxygen extraction in muscle tissue for the case of static muscle contraction, these methods are not compatible with dynamic exercise and the reported temporal resolutions ($>5\text{s}$) may be insufficient to capture peak values and off-kinetics following dynamic exercise, even for the case of a single imaging slice.

An alternate approach to estimate oxygen consumption is to measure flow and oxygen saturation in large conduit veins to integrate whole muscle utilization of oxygen. This approach has been used in conjunction with invasive catheterization in several landmark studies (9-11), and more recently using MRI in muscle (22, 23) and the brain (24, 25). Specifically, MRI studies have utilized the magnetic susceptibility shift of deoxyhemoglobin (22, 24, 25) as an oxygen saturation contrast mechanism, which can be imaged relatively quickly, particularly in the blood pool. However, no previous studies have considered the effects of dynamic exercise with the rate of consumption of oxygen (VO_2) as a targeted parameter.

In the current study we developed and evaluated a variant of the interleaved oxygen consumption imaging method from Langham et al. (22, 23, 26, 27) to enable rapid imaging of venous blood flow (VBF) and venous oxygen saturation (SvO₂) in conjunction with dynamic exercise. The method was designed to emulate invasive studies that have targeted simultaneous venous blood flow and oxygen saturation to assess whole muscle oxygen consumption (9-11). Our specific aims were to determine the feasibility and reproducibility of this approach in the femoral vein in conjunction with knee extensor exercise, isolating the quadriceps muscles, within the MRI scanner bore. Specific targeted quantitative measurements include flow (VBF) and oxygen saturation (SvO₂) in the femoral vein at the time of peak exercise and dynamically during the subsequent recovery, for determination of peak dynamic exercise VO₂ and the recovery time constant of VO₂ for the assessment of off-kinetics.

Methods

Subjects

Nine healthy male subjects (31±6 yrs., 177±6 cm, 80±10 kg), with no prior history of cardiovascular disease, provided written informed consent following an institutional review board-approved protocol.

Exercise Device

A custom-built MRI-compatible knee-extension ergometer was used for dynamic exercise, which consists of an adjustable A-frame knee support and a hanging adjustable weight. A boot system connects the weight to the subject's foot by a cable. A 12 cm vertical displacement, Δd , of a weight, $m = 5$ kg, and a knee-extension repetition period of $\Delta t = 1.2$ seconds was used to achieve a targeted average power of ~5 watts ($P_{ave} = m * g * \Delta d / \Delta t$, where $g = 9.81$ cm/s² is acceleration due to gravity). An audio click track sent to the subject's headphones was used to maintain the knee-extension repetition rate during exercise. The ergometer was designed to allow subjects of a wide range of heights to exercise within the

specified range of motion with the targeted femoral vein location at the magnet isocenter (60 cm bore, 1.5T Siemens Sonata, Siemens Healthcare, Erlangen, Germany).

Imaging of Venous Oxygen Saturation

Magnetic resonance susceptometry estimation of oxygen saturation (oximetry) relies on the difference in magnetic susceptibility, ΔX_{do} , between deoxygenated intravascular blood and the surrounding tissue, which gives rise to directly measurable shifts in the magnetic field (24, 25). For whole blood, the susceptibility shift can be expressed as a function of hematocrit, Hct , and the fraction of oxygenated hemoglobin, HbO_2 , according to $\Delta X = \Delta X_{do} Hct(1-HbO_2)$, where $\Delta X_{do} = 4\pi \cdot 0.27$ ppm is the susceptibility difference between fully deoxygenated and fully oxygenated red blood cells in SI units. Previous studies have differed on the susceptibility shift of oxygenated and deoxygenated blood (16, 28-31) with the strongest support for a value of 0.27 ppm (32). For a given susceptibility shift, the corresponding shift in magnetic field can be estimated using a long paramagnetic cylinder model according to $\Delta B = 1/6 \cdot \Delta X \cdot B_0 \cdot (3\cos^2\theta - 1)$ (33, 34), where θ is the vessel tilt, or the angle between the vessel long axis and the main field, B_0 . The shift in magnetic field, ΔB , can be measured using the phase difference between images at two echo times, such that $\Delta B = (\varphi(TE_1) - \varphi(TE_2)) / (\gamma \Delta TE)$, where $\Delta TE = TE_1 - TE_2$ and γ is the ¹H gyromagnetic ratio ($\gamma = 42.576$ MHz/T). The muscle reference tissue is assumed to have a susceptibility that is similar to fully oxygenated arterial blood (35). Then, by combining expressions for ΔX and ΔB , the oxygen saturation in a vessel can be estimated as:

$$HbO_2(\%) = 100 * \left\{ 1 - \frac{2 * |\Delta\varphi / \Delta TE|}{\gamma * \chi_{do} * Hct * B_0 * (\cos^2\theta - 1/3)} \right\} \quad \text{Eq. 2.1}$$

where $Hct = 0.43$ was assumed for all subjects in this study. Thus, the venous oxygen saturation, $SvO_2 = HbO_2$, can be estimated using only the measured phase difference between two images acquired in a multi-echo acquisition, $\Delta\varphi$, and the vessel tilt, θ . Similar to Langham et al., the effects of the static field inhomogeneity,

which are additive to the targeted susceptibility shift in the vein, were measured and removed by fitting the phase difference images to a second order polynomial surface in a user-defined region surrounding but excluding the vessel region (33). The median SvO_2 value from within the vessel was reported in this study. A schematic of the multi-echo pulse sequence used for evaluation of SvO_2 used is shown in Fig. 2.1.

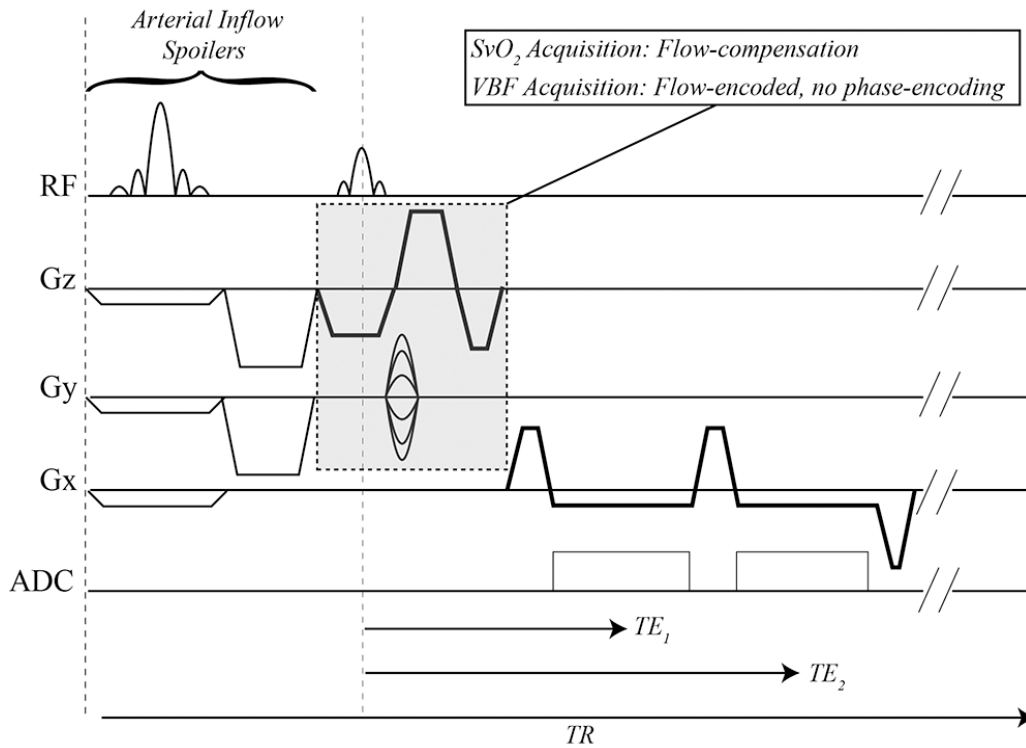


Figure 2.1 – A schematic of the multi-gradient-echo pulse sequence used for evaluation of venous oxygen saturation (susceptometry) and complex-difference imaging of blood flow. For both acquisitions, a spatial saturation pulse (slice prescription detailed in Fig. 2.5) is applied in every TR to minimize signal from the arterial blood pool and to reduce the imaging field of view. For susceptometry acquisitions, flow-compensation is applied in the slice-encoding direction. The same sequence and slice prescription are used for complex-difference blood flow acquisitions, but without the application of phase-encoding gradients, and with interleaved application of differentially flow-encoded gradients in the slice-encoding direction, in each sequential TR. The protocol for susceptometry and complex-difference blood flow acquisitions in conjunction with baseline and exercise studies is detailed in Fig. 2.3.

Complex-difference Flow Imaging for Estimation of Venous Blood Flow (VBF)

A complex-difference projection method was used for real-time imaging of VBF (36). Phase-encoding gradients are turned off in order to yield a projection of the imaging slice in the phase-encoding direction with every readout. The complex-difference method is based on the subtraction of MRI signal projections from sequential TRs to remove signal from stationary tissue. The application of differential flow encoding in the slice-selection direction between the sequential projections yields signal from moving spins within the vein with a magnitude that is proportional to flow (36). A schematic of the pulse sequence used for evaluation of VBF is shown in Fig. 2.1. The equation relating the complex-difference signal and flow at each location in the projection, x , can be expressed as:

$$F(x) = \frac{S_{CD}(x) * V_{enc} * \Delta V}{\pi * S_0 * \Delta z} \quad \text{Eq. 2.2}$$

where $F(x)$ is the voxel flow rate in ml/s at the location x in the projection, $S_{CD}(x)$ is the magnitude of the complex-difference signal at x , V_{enc} is the encoding velocity in cm/s, S_0 is the signal intensity in the vein from a reference image, ΔV is the voxel volume in the image used to measure S_0 , and Δz is the slice thickness. This expression was previously derived and validated (36). A step-by-step description of the complex-difference processing to yield a signal in units of flow in the current study is detailed below, and also outlined in Fig. 2.2.

- 1) The complex-difference projection signal, $S_{CD}(x)$, was measured as the complex subtraction of the flow-encoded and flow-compensated acquisitions for each pair of sequential acquisitions. The delay between projection acquisitions is TR = 30 ms. 2.2B shows a typical $S_{CD}(x)$ profile over the vein at peak flow immediately post-exercise.
- 2) The phase of the complex-difference signal, θ_{CD} , has contributions from radio-frequency coils, off-resonance, magnetic susceptibility and velocity-encoded phases. $S_{CD}(x)$ was phase-corrected by determining the phase angle at which the

real component of the projection within the vessel region is a maximum. A single value for θ_{CD} was used for all pixels in the projection and was recalculated for each complex-difference subtraction pair over time, to account for motion and changes in velocity over time. Analysis of the phase-corrected real data, as opposed to the absolute value of the projection, was necessary to retain the phase relationship between residual background signal and the signal from the vein, as illustrated in Fig. 2.2B.

- 3) Residual background signal in the phase-corrected real projection, due to incomplete subtraction of stationary tissue, was removed by measuring the signal intensity over the projection, excluding the vessel region, and subsequently interpolating the residual signal over the vessel prior to subtraction of the residual. Fig. 2.2C shows removal of the background signal from 2.2B, and why phase-corrected real data is necessary to avoid underestimation of flow (Fig. 2.2E).
- 4) The complex-difference method requires reference signal intensity, S_0 , from the venous blood pool to convert the magnitude of the complex-difference signal, S_{CD} , to units of flow (36). The reference signal was acquired using the first echo of the SvO_2 acquisitions, which were designed to have identical acquisition pulse sequence parameters to the complex-difference acquisition save for the inclusion of phase-encoding gradients, as shown in Fig. 2.2. S_0 was measured as the average signal intensity over the vessel lumen and the average over time, normalized by the number of phase-encoding lines in the acquisition, to account for scaling of the Fourier transform. Fig. 2.2D shows a typical sample S_0 signal intensity over time, for a post-exercise experiment, and the selection of S_0 .

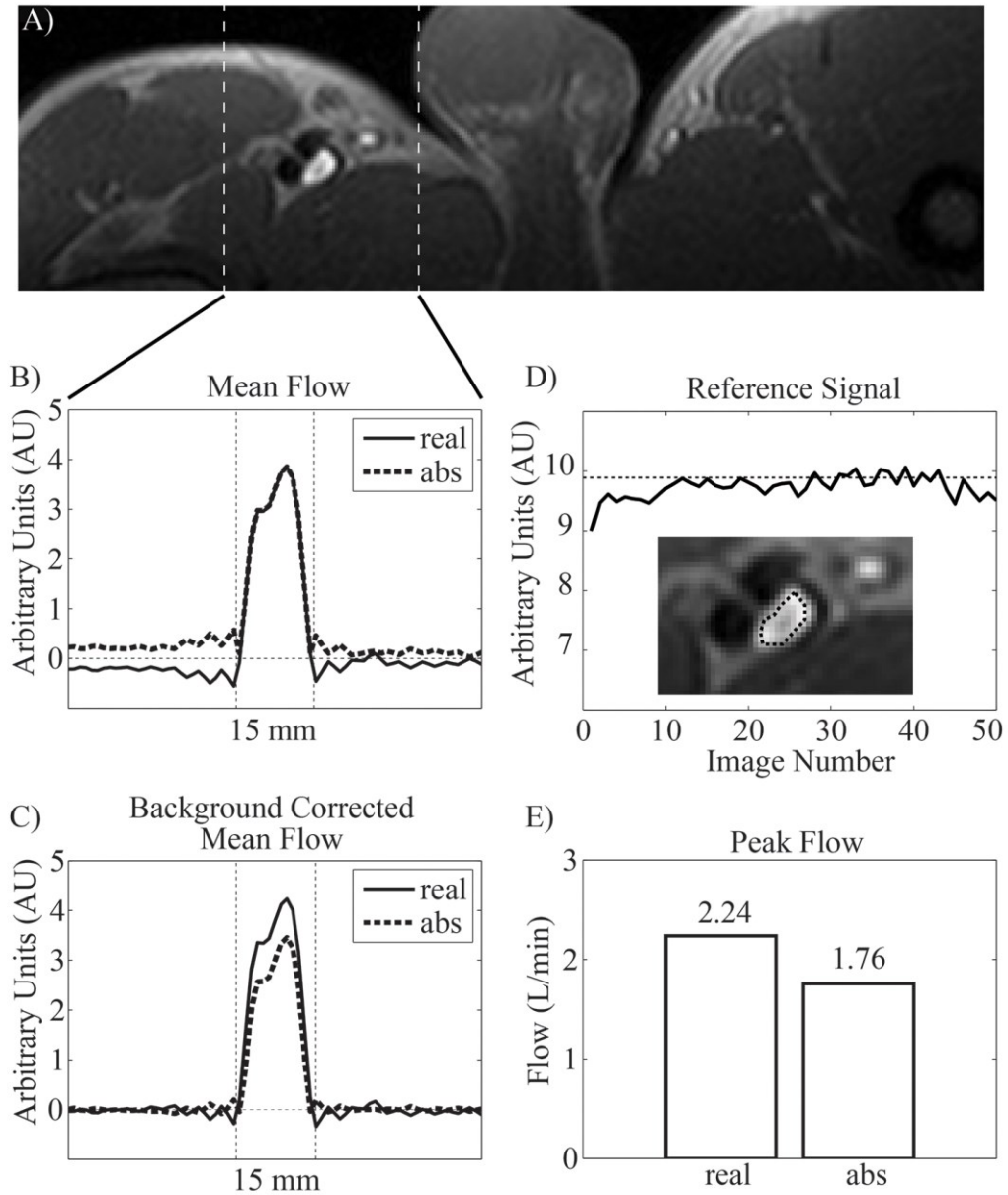


Figure 2.2 – A) Magnitude image showing a cross-section of femoral vein from one of the subjects. Raw complex-difference data is shown as both phase-corrected real and absolute signal intensities, B) before and C) after correction of the background signal. The mean signal intensity in the vessel from the magnitude images acquired over 50 acquisitions (dashed line) for calculation of the reference signal S_0 is shown in D). Peak venous flow from this subject, using both the phase-corrected real and absolute complex-difference signals, is shown in E), illustrating the potential for underestimation of flow if absolute values are used.

Pulse Sequence

As shown in Fig. 2.1, the same pulse sequence template, with identical TE, TR, radiofrequency pulses, saturation pulses and slice selection and frequency-encoding gradients was used for both complex-difference (VBF) and susceptometry (SvO₂) acquisitions. The interleaved sequences were implemented on a 1.5T MRI scanner (Sonata; Siemens Healthcare; Erlangen, Germany). A flexible single element surface coil was used for signal reception and the body coil was used for excitation. Acquisition parameters for the susceptometry acquisitions were 5 mm slice thickness, 192x80 acquisition matrix, 384 x 160 mm field of view, 2 mm in-plane resolution, 260 Hz/pixel receiver bandwidth, TR/TE₁/TE₂ = 30ms/5ms/10ms, flip angle = 20°, flow-compensation in the slice-selection direction, with 2.4 seconds acquisition time per image for 80 k-space lines. Complex-difference acquisition parameters were identical to the SvO₂ acquisitions, but with no phase-encoding gradients and a velocity encoding strength of $V_{enc} = 170$ cm/s, which was implemented as flow-encoded slice-oriented gradients with equal and opposite first moments. Each complex-difference acquisition consists of 40 pairs of projections (to match the 80 lines of k-space in the SvO₂ acquisition) that were acquired within the 2.4 second imaging window, with each pair of acquisitions spanning a real-time temporal window of $2 \cdot TR = 60$ ms.

To visualize the venous anatomy, an arterial saturation venogram was acquired with the following parameters: 40 slices, 3 mm slice thickness with no gap, 256x176 acquisition matrix, 400x275 mm field of view, 260 Hz/pixel receiver bandwidth, TR/TE = 24 ms/3.57 ms, flip angle = 40°, with a gradient echo readout and a total scan time of 150 seconds. A superior saturation pulse was applied with every TR to eliminate signal from the arteries, to allow for clear identification of the veins. Acquisitions for muscle mass calculations used a single shot fast spin echo sequence with 50 slices and 10 mm slice thickness with no gap, 192x96 acquisition matrix, 400x250 mm field of view, 300 Hz/pixel receiver bandwidth, TR/TE = 287 ms/30 ms for a total scan time of 29 seconds.

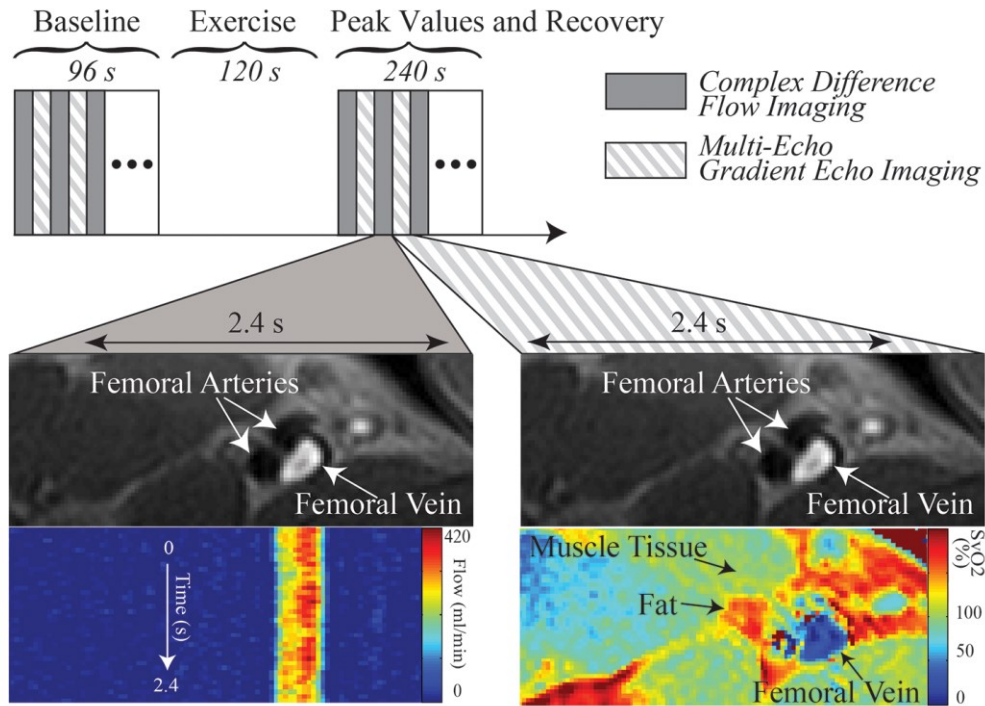


Figure 2.3 – Rest and exercise study protocol illustrating the interleaved complex-difference flow imaging and susceptometry imaging, each of which has a temporal acquisition window of 2.4 seconds. 40 independent measurements of flow are obtained in the 2.4-second window (bottom left) and a single venous oxygen saturation image is acquired in the sequential window (bottom right). This sample data corresponds to the first imaging windows (the first 4.8 seconds) post-exercise in a representative subject.

Exercise and Imaging Protocol

As shown in Fig. 2.3, susceptometry acquisitions were interleaved with complex-difference flow acquisitions, with typical imaging times of 2.4 seconds for each acquisition. Using the arterial saturation venogram, care was then taken to prescribe the imaging slice for VBF and SvO_2 experiments perpendicular to the long axis of the vein and in a location proximal to the femoral circumflex veins, but distal to the junction of the femoral vein and greater saphenous vein, as shown in Fig. 2.4.

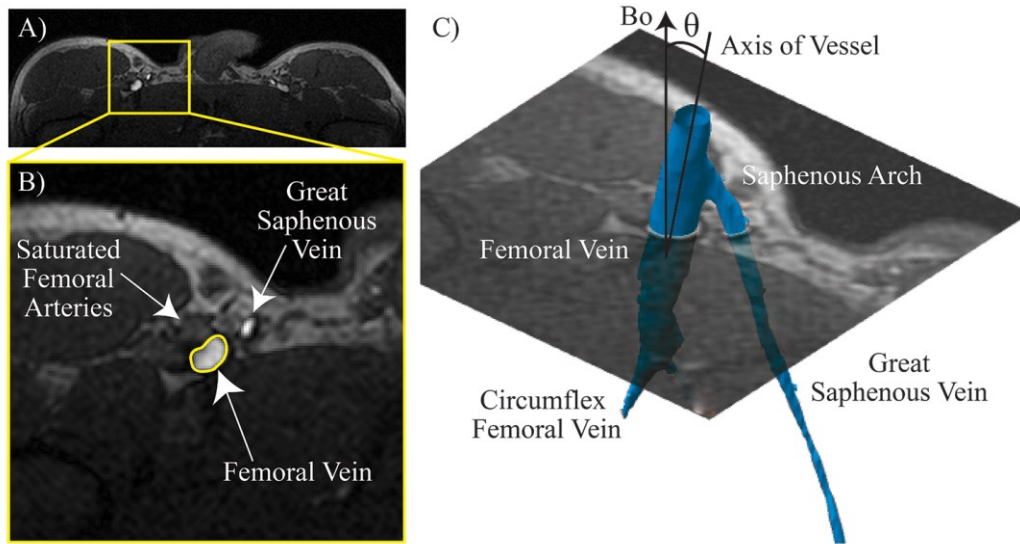


Figure 2.4 – A) Transverse plane cross-section magnitude image showing the femoral vein location, and B) a zoomed magnitude image showing the outlined femoral vein and the great saphenous vein and with saturated signals in the femoral arteries. C) A 3 dimensional model reconstruction from the venogram scan showing the location of imaging slice in relation to the saphenous arch and the circumflex femoral vein. This figure also illustrates the calculation of the angle, θ , which is the angle between the main static magnetic field, B_0 , and the vessel.

Additionally, the imaging slice location was selected to provide sufficient muscle reference tissue for the determination of background off-resonance frequency (107). For all VBF and SvO_2 imaging studies, a slab-selective saturation pulse (15 cm slice thickness) was applied proximal to the imaging slice, in every TR, both to saturate the signal from the inflowing arterial blood and to provide a field of view reduction to reduce image acquisition time by saturating the signal posterior to the vein and reference muscle tissue. Suppression of the arterial blood signal was necessary to eliminate artifacts from pulsatile flow over the 2.4 second imaging window for SvO_2 acquisitions and to enable the complex-difference projection flow imaging method used to estimate VBF, which could otherwise be contaminated by potentially overlapping arterial blood flow (77, 134). Fig. 2.5 illustrates the prescription of the imaging slice and the orientation of the saturation slab.

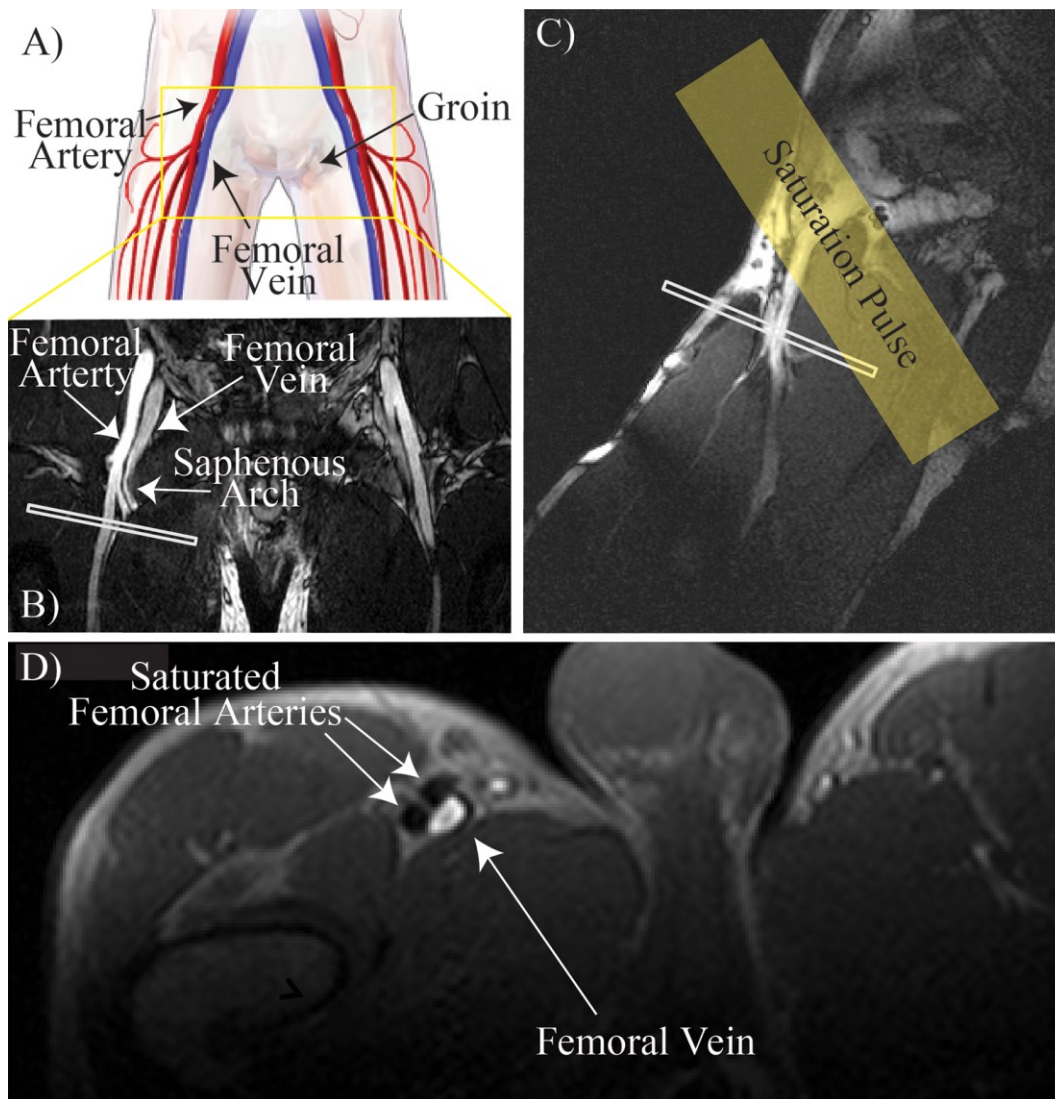


Figure 2.5 – Slice Prescription Details. A) Sketch of lower limb vasculature illustrating the location of the femoral vein. B) Coronal magnitude image showing the femoral arteries and veins, as well as the saphenous arch. The imaging plane is prescribed distal to the saphenous vein bifurcation. C) Sagittal plane magnitude images used to define a slice location, and direction perpendicular to the length of the femoral vein. This image is also used to prescribe the saturation pulse that will remove arterial blood signal, and reduce the effective field of view. D) Resulting transverse plane cross-section image showing the femoral vein and the saturation in the arterial blood signal and the lower half of the image.

All subjects performed two repeated 2-minute, 5-Watt knee-extension exercise bouts, separated by a 10-minute recovery period. Fig. 2.3 outlines the baseline and post-exercise imaging windows used for all studies in conjunction with the timing of the exercise bouts. Motion during exercise precluded the acquisition

of data during the exercise bouts but the peak flow and recovery acquisition began immediately (<1 second) with the cessation of exercise.

Measurement of Skeletal Muscle Oxygen Consumption

Similar to previous invasive (9-11) and non-invasive imaging studies (29), skeletal muscle oxygen consumption, VO₂, was estimated using Fick's principle as the product of the venous blood flow (VBF), which is a surrogate for the whole muscle blood flow, and the arteriovenous oxygen difference, $a-vO_{2(diff)}$, as shown in Equation 3.

$$VO_2 = VBF * a-vO_{2(diff)} = VBF * Ca * Hgb * (SaO_2 - SvO_2) \quad \text{Eq. 2.3}$$

The $a-vO_{2(diff)}$ was estimated as the product of the oxygen carrying capacity per gram of hemoglobin, $Ca = 1.34 \text{ mL O}_2/\text{g Hb}$, the assumed typical hemoglobin level, $Hgb = 14.6 \text{ g/dL}$ (with a hematocrit (Hct) of 0.43), and the difference between arterial oxygen saturation, SaO_2 , measured from a finger pulse oximeter and assumed constant during the exercise bouts, and SvO_2 , as estimated from MR oximetry experiments (38).

Vessel Tilt Calculation

The three-dimensional venogram, as shown in Fig. 2.4, was used for calculation of the femoral vein angle, θ , relative to the magnet bore. The vessel was traced with an automated region-tracing algorithm based on signal intensities, and the centroid of the vessel along its length was used to define the angle of the vessel with respect to the main field at the location of flow and oximetry imaging slice.

Muscle Mass Quantification

The mass of the quadriceps muscle, measured from volumetric anatomical images, was used to index venous blood flow and skeletal muscle VO₂ to the mass of knee-extension targeted muscle groups. A single-shot fast spin echo sequence was used to image the thigh muscles groups from the knee to groin. A region containing quadriceps muscle was traced on each slice. The volume contained

within this 3D region was multiplied by 1.06 g/mL to provide an estimate of the muscle mass.

Time-Course Experiments and Data Analysis

As shown in Fig. 2.3, the pair of interleaved complex-difference flow and oximetry experiments, each with duration of 2.4 seconds, were repeated 20 times over 96 seconds at baseline, and 50 times over 240 seconds post exercise. Imaging began simultaneously (within 1 second) with the completion of exercise. For moderate intensity exercise, the VO₂ kinetics are well described by a simple mono-exponential function (39), $SvO_2(t) = SvO_{2(\text{offset})} + A \cdot \exp(-t/\tau)$, where $SvO_{2(\text{offset})}$ is a baseline offset value, A is scaling factor and τ is the time constant. For all subjects, the VO₂ recovery time course data for each exercise bout was fit with a mono-exponential function to estimate the recovery time constant, τ .

Reproducibility and Statistical Analysis

Test-retest reliability was measured by repeating the imaging protocol and exercise trial, as shown in Fig. 2.3, with a 10-minute recovery interval. Reproducibility was assessed using linear correlation, coefficient of variation (CV), and interclass correlation (ICC) for peak post-exercise VBF, SvO₂ and VO₂, and time constant of recovery of VO₂ between the two trials.

Results

The mean quadriceps muscle mass was 2.43±0.31 kg and the mean arterial oxygen saturation, from the pulse oximeter, was 97.7±0.6%. The mean femoral vein tilt with respect to the B₀ field was 22.1±2.6 degrees.

Figure 6A shows a typical view of the femoral vein cross-section for flow and SvO₂ experiments, with a zoomed view in 7B, from a sample multi-echo gradient-echo acquisition, post exercise. The good saturation of the arterial blood pool signal shown here was observed in all subjects at all time frames in baseline and post-exercise scans. Sample SvO₂ maps, corresponding to the image frames immediately post exercise and at baseline, are shown in 6C and 6E, and a time-

series of 40 complex-difference projections, spanning 2.4 seconds, immediately post exercise is shown in 6D. Flow waveforms for the 50 acquisitions post-exercise for this subject are shown in 6F. Cardiac pulsatility can be seen in the venous flow data in 6D and F.

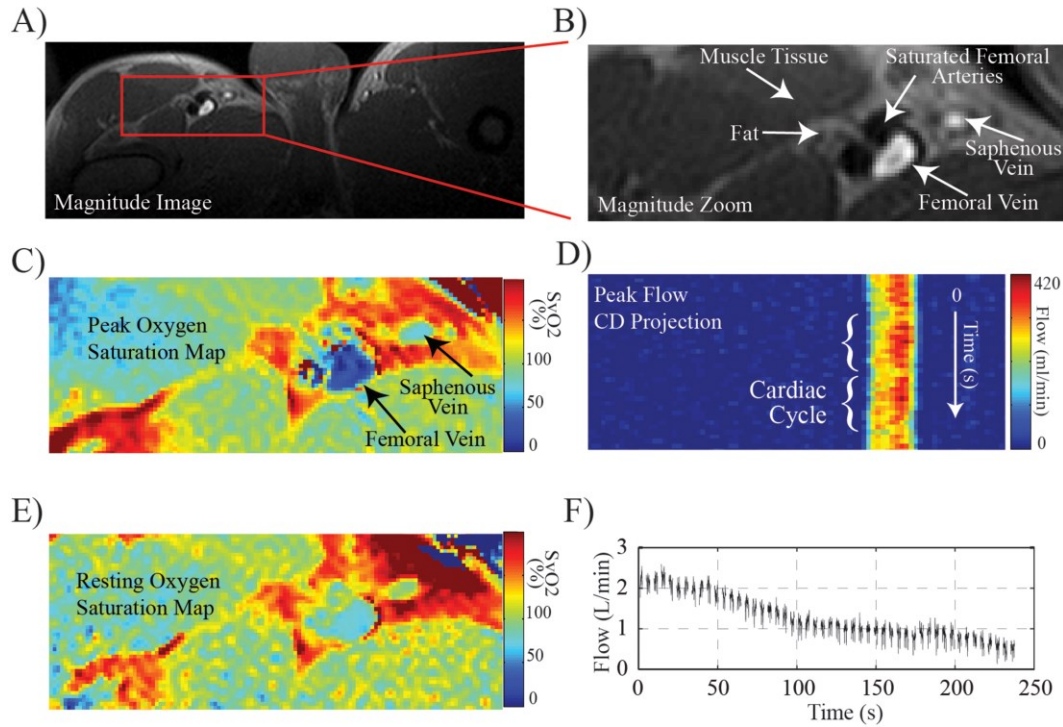


Figure 2.6 – Sample imaging results. A) Magnitude image showing a typical slice orientation perpendicular to the targeted femoral vein. B) Zoomed magnitude image showing the location of the femoral vein and the saturation of the femoral artery signal. C) and E) show the oxygen saturation map (% SvO_2) for peak post-exercise and resting, respectively. A series of 40 flow projections, acquired over a 2.4 second window immediately post exercise is shown in D), and F) shows the flow waveforms over the 4 minute recovery period post-exercise, where the pulsatile flow over the cardiac cycle is visible, as indicated in D). Resting flow in this subject was 0.2 L/min.

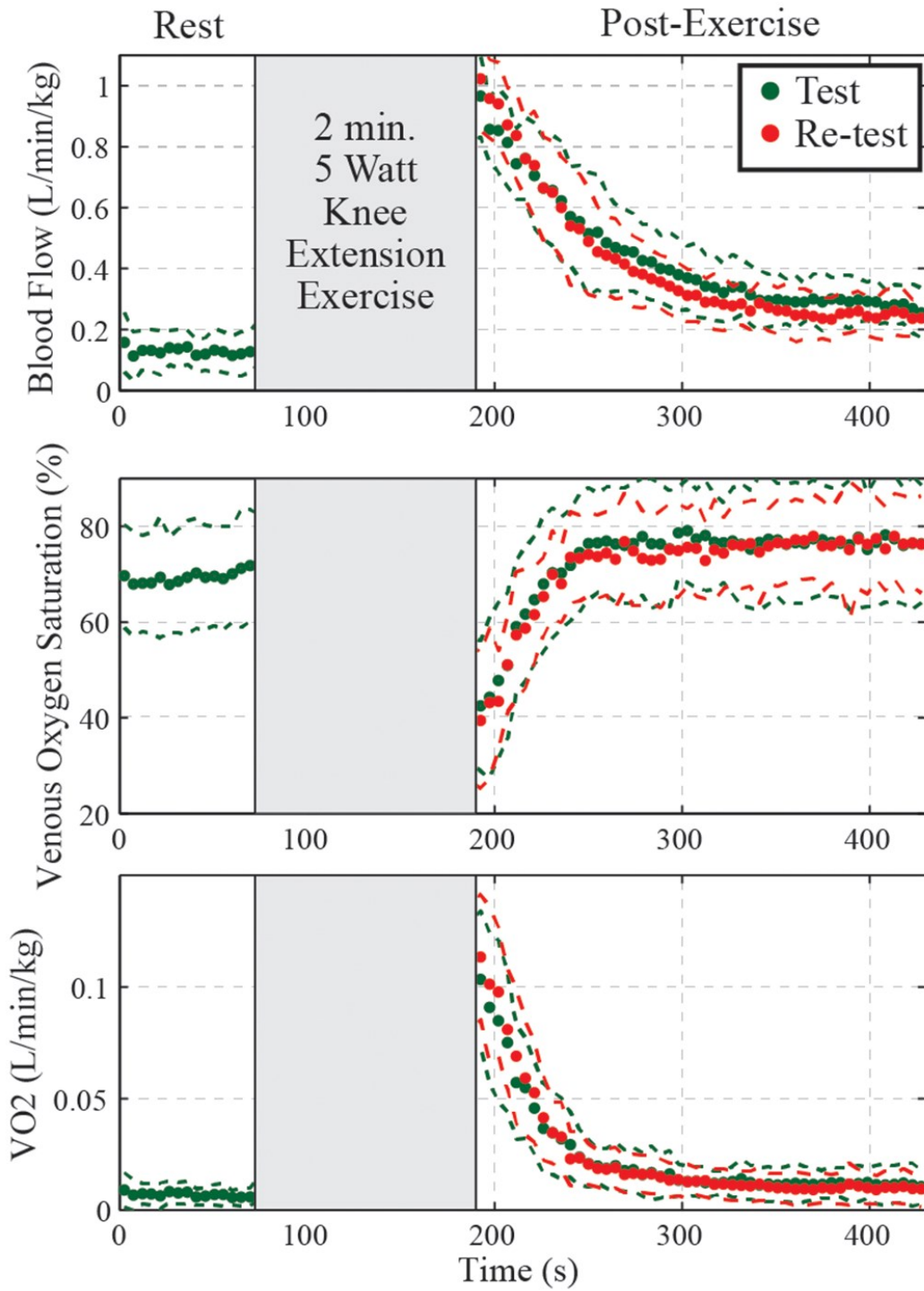


Figure 2.7 – Test and Re-test group average data of normalized venous blood flow (VBF), venous blood oxygen saturation (SvO₂) and oxygen consumption (VO₂) time course data in all subjects at rest for 96 seconds, and for 240 seconds starting immediately following 2 minutes of 5 Watt knee extension exercise. Mean data is shown as solid points. Dashed lines indicate one standard deviation over the study population.

Figures 7A, 7B and 7C show the average time-course data for all subjects, for femoral vein blood flow, SvO₂ and VO₂, for both test and re-test acquisitions. The dashed lines indicate one standard deviation. Figure 8 shows the correlations between the test and retest acquisitions for peak flow (R²=0.69), SvO₂ (R²=0.77), VO₂ (R²=0.78) and recovery time constant (R²=0.85). Figure 9 shows the correlation between the quadriceps muscle mass and venous oxygen saturation at peak exercise (R²=0.74) and corresponding peak VO₂ (R²=0.76), but without a significant correlation to peak flow (R²=0.14). Table 1 summarizes all other measured parameters. All data are reported as mean ± standard deviation.

Table 2.1: Group Mean Data

	Baseline 1	Baseline 2	Post Ex. 1	Post Ex. 2	CV(%) / R / ICC
SvO₂ (%)	69.4±10.1	68.0±9.3	43.2±13.5	40.9±13.1	15.6 / 0.88/ 0.88
VBF					
(L/min)	0.31±0.15	0.37±0.13	2.20±0.27	2.41±0.31*	7.6 / 0.83 / 0.68
(L/min/kg)	0.13±0.06	0.14±0.05	0.91±0.12	1.00±0.16*	-- / -- / --
VO₂					
(ml/min)	16.7±10.5	19.9±4.1	236.4±65.3	266.2±57.3 *	12.3 / 0.88 / 0.80
(ml/min/kg)	6.8±4.1	8.4±1.6	95.7±18.0	108.9±17.3 *	-- / -- / --
τ (s)	--	--	26.1±3.5	26.0±4.0	6.0 / 0.92 / 0.92

*p < 0.05 between test and re-test. SvO₂ – venous oxygen saturation in the femoral vein, VBF – blood flow in the femoral vein, VO₂ – rate of oxygen consumption.

Discussion

The current study has demonstrated the feasibility and good test-retest reproducibility of a novel MRI method for the measurement of venous blood flow and venous oxygen saturation, for the estimation of skeletal muscle oxygen consumption, VO₂. Conventional expired gas analysis of VO₂ with whole body exercise does not distinguish the cardiac and skeletal muscle limitations to exercise performance, particularly in patients with impaired heart function (40, 41). Isolated muscle exercise, with quantification of oxygen consumption in the isolated limb, removes the cardiac limitations and allows for targeted skeletal muscle studies. The quadriceps muscle was targeted in the current study as it can be isolated with dynamic single leg knee extension exercise and quadriceps muscle function is representative of an individual's capacity for exercise (40, 42).

The temporal resolution of the proposed method was sufficient to measure venous blood flow, venous oxygen saturation, and skeletal muscle VO₂ immediately following knee-extension exercise (targeting the quadriceps muscle) as well as the dynamics of all parameters, to determine the time constant of VO₂ recovery following exercise. The immediate post-exercise values in the current study are in general agreement with peak exercise values from previous reported invasive studies at similar workloads using catheter-derived venous blood flow and oxygen saturation values post knee-extension exercise (10). The muscle VO₂ time-constant of recovery is similar to previously reported expired gas VO₂ time-constant for younger males during dynamic isolated muscle exercise (39, 43).

On average, peak flow values increased ~7 fold over baseline and venous saturation dropped by ~25% (approximately doubling a-vO_{2(diff)}) for a resulting increase in oxygen consumption by ~15 fold with exercise. For reproducibility studies, the baseline values for VBF, SvO₂ and VO₂ differ slightly, although they are not statistically significant (Baseline 1 and Baseline 2 in Table 2); the second showing marginally increased blood flow, decreased venous oxygen saturation, and thus increased oxygen consumption. These small changes towards increased flow and rate of oxygen consumption may be due to the relatively short 10 minute rest

periods between tests which may be insufficient to allow the subjects to return to homeostasis. However, both baseline femoral vein SvO_2 studies have values that are similar to previous invasive studies in large groups of healthy subjects (44). Similarly, the post exercise peak flow values are very similar but slightly higher in the second trial, venous saturation is slightly lower, and thus VO_2 is slightly higher. Again, this may reflect incomplete recovery to homeostasis at the onset of exercise in combination with a relatively short exercise interval of 2 minutes, which may not have been sufficiently long to reach steady state or peak values at the prescribed workload. As shown in Fig. 2.7, the average time-course of flow, oxygen saturation, and VO_2 over all subjects are nearly identical in the test and re-test studies. The time-constant of VO_2 recovery, calculated from a best-fit mono-exponential decay of VO_2 , had the lowest coefficient of variation of all parameters at 6%.

As shown in Fig. 2.8, there is wide range of peak VO_2 values in the 9 healthy young subjects, and, as expected, Fig. 2.9C shows that these values are significantly correlated to quadriceps muscle mass. Interestingly, as shown by Figs. 2.9A and 2.9B, the increased VO_2 with larger muscle mass is due largely to increased oxygen extraction (lower SvO_2) and not to increased flow. However, all subjects performed the same absolute exercise work of $\sim 5\text{W}$ which is likely not the same fraction of their peak workload, and thus these differences could be related to differences in relative workload. Future studies using this methodology would ideally determine each subject's peak load, and have exercise performed at known fractions of this peak, as is the standard for whole body exercise testing.

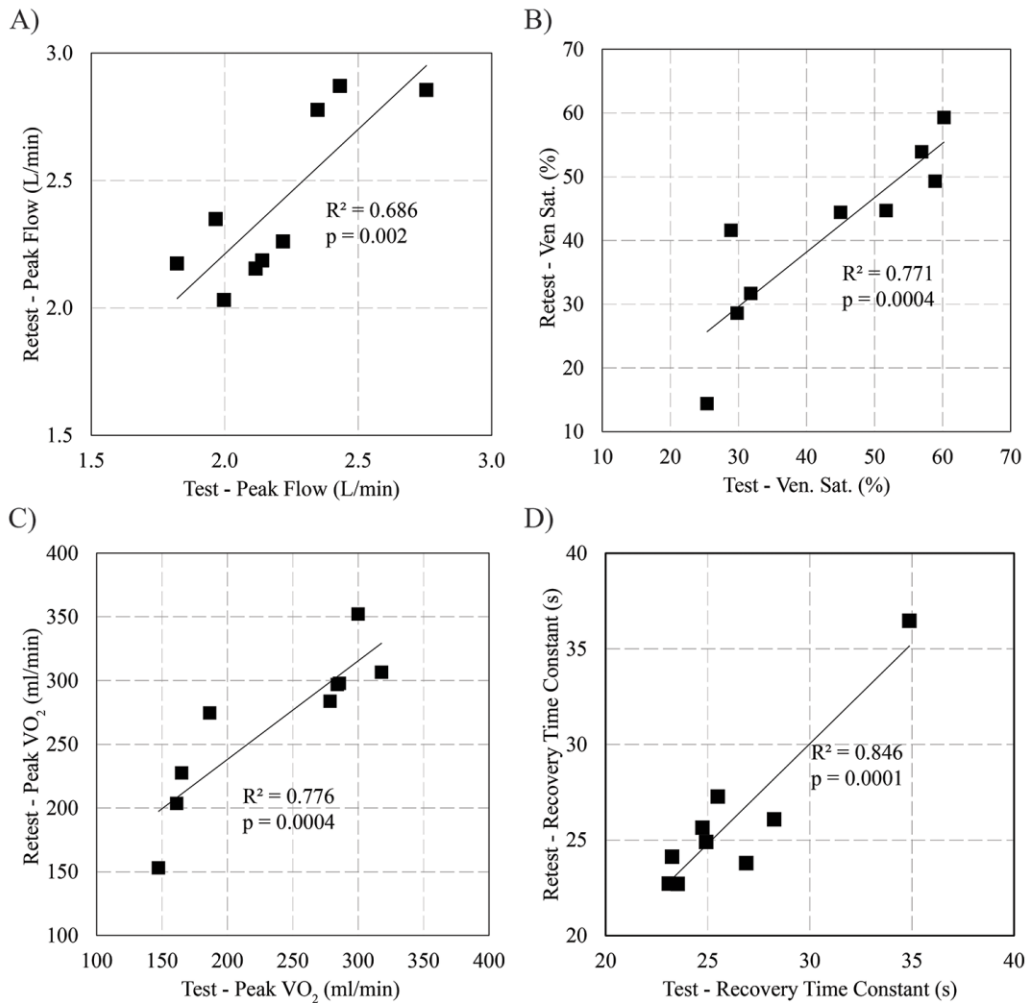


Figure 2.8 – Test-retest correlations for all parameters immediately following exercise: A) blood flow (VBF), B) venous saturation (SvO₂), C) oxygen consumption (VO₂), and D) VO₂ recovery time constant, τ .

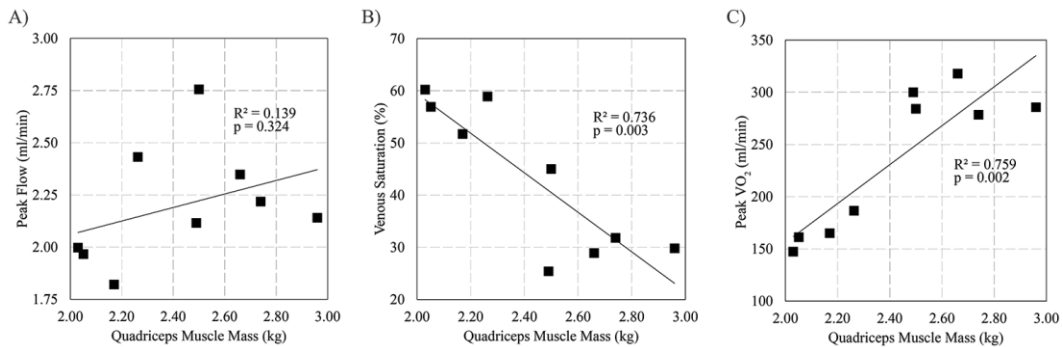


Figure 2.9 – Correlations between quadriceps muscle mass and each of A) blood flow (VBF), B) venous oxygen saturation (SvO₂) and C) oxygen consumption (VO₂) for peak values measured immediately after exercise.

Experimental Considerations

With the proposed method, the quadriceps muscle blood flow, oxygen extraction and oxygen consumption with exercise are estimated based on the flow and oxygen content of the blood in femoral vein. Thus, the location of the imaging slice along the femoral vein is an important experimental factor. Longer cylindrical sections of vein are desirable as they are more likely to meet the geometric assumptions of the susceptometry model (33, 34). Also, too high (superior) of a location along the vein is more likely to include venous blood that was not utilized by the quadriceps, for example from the great saphenous vein. Too low (inferior) of an imaging location, towards the circumflex, will result in increasingly complex branching of the femoral vein which will affect the flow quantification and a smaller exercising muscle mass will be reflected. However, MRI provides detailed vein and muscle morphology on a subject-by-subject basis, so that slice prescriptions can be routinely optimized, as shown in Fig. 2.4.

The effects of pulsatility, in both the targeted femoral vein and arteries, was a critical factor in designing the methods presented in this study. Large temporal variations in signal over the cardiac cycle, from inflow signal enhancement, gave rise to significant flow-related artifacts in the phase-encoding direction, particularly from the arteries. These artifacts confounded quantitative measurements in the neighboring femoral vein. Saturation of the arterial signal, using a superior saturation band as shown in Fig. 2.5, was necessary to ensure no contamination at the location of the femoral vein. Additionally, pulsatility of the femoral venous blood flow necessitated use of real-time imaging to avoid similar artifacts in the venous flow imaging. Conventional single-shot phase-contrast imaging in the femoral vein consistently yielded flow-related artifacts and large errors in peak flow following exercise. These artifacts could be avoided with gated-segmented imaging to resolve flow over the cardiac cycle at the expense of drastically reduced temporal resolution that would not be compatible with dynamic exercise studies. The real-time complex difference approach reported in the current study overcame these limitations. Finally, while imaging studies began immediately after exercise, there

was still significant bulk motion of the recovering muscles over a period of tens of seconds following the cessation of exercise, and thus imaging windows had to be sufficiently short to avoid blurring and contamination of the vessels by the surrounding lipids. The imaging window durations of 2.4 seconds for venous oxygen saturation and 60 ms for venous flow were sufficient to minimize flow related and bulk motion artifacts in all subjects in the current study, at rest and post-exercise.

Limitations

We acknowledge that the methods used in this study provide no insight into the spatial variations of flow, oxygen extraction, or estimated VO_2 within muscles groups that could be provided with direct imaging of these parameters in the muscle tissue. However, current MRI methods for estimation of tissue perfusion with simultaneous oxygen saturation do not provide sufficient temporal resolution and spatial coverage to determine the whole muscle oxygen consumption responses to dynamic exercise. No previous MRI study to our knowledge has illustrated imaging of these parameters, even in a single imaging slice, in conjunction with dynamic exercise. Additionally, given the heterogeneous patterns of quadriceps muscle flow with exercise (13), single-slice imaging is likely insufficient to reflect the whole muscle response to exercise.

An important limitation of methods proposed in the current study is the potential effects of mixing of the venous blood pools from the targeted quadriceps muscle and from the regions distal to the muscle, in the calf and foot. This mixing will lead to overestimation of the true quadriceps flow, and venous oxygen saturation values will underestimate the drop in SvO_2 during exercise due to mixing with higher oxygen saturation venous blood pools from distal non-exercising muscles. Previously, these effects were mitigated in invasive studies using a similar venous blood pool method by placing a cuff placed below the thigh, which was inflated just prior to data collection to eliminate distal blood flow from the femoral vein (9, 10). A similar approach could be combined with the methods present here.

Another potential limitation of the method is the requirement for a large caliber femoral vein, which could be obscured with conditions such as deep vein thrombosis. Additionally, the susceptometry method relies on reference muscle tissue near or surrounding the targeted vessel; a lack of tissue near the vein will confound the estimation of blood oxygen saturation based on the relative shift in the magnetic susceptibility. Finally, the method relies on the geometric assumption of a long cylindrical vessel, and the impact of the range of actual venous geometries on a person-by-person basis is unknown. None of these factors limited the current study of healthy younger subjects and future patient-oriented studies will be necessary to determine the relative importance of these potential confounders.

Additional assumptions were made in the current study that could be avoided in the future. Blood samples for our subjects were not available for our subjects so a hemoglobin value of 14.6 g/dL and a hematocrit of 0.43 were assumed for all subjects. Also, femoral artery oxygen saturation was assumed to be consistent with pulse oximetry measured saturation, and it was assumed to be constant over the short exercise trial, which is well justified for moderate isolated muscle exercise.

A final limitation of the current study is that there is no direct measurement of the true work being performed by the subject; the true distance of the mass displacement for each knee-extension was not measured and the internal friction of the system was not taken into account.

Conclusion

Simultaneous femoral vein blood flow and oxygen saturation measurements are feasible and reproducible immediately post-exercise, and subsequently during the period of off-kinetics, for the estimation of whole muscle VO_2 . Our resting values, peak values and time course data during recovery are in general agreement with previous reported values from invasive hemodynamic knee extension studies. In future studies, simultaneous measurement of blood flow and SvO_2 will enable the independent consideration of these physiologic factors as mechanisms of impaired VO_2 in subjects with reduced exercise capacity, independent of impaired

heart function. When combined with cardiac and vascular studies, these methods can investigate the relative importance of the mechanisms that contribute to reduced exercise capacity in common conditions including those at risk for or with heart failure.

Chapter 2 References

- [1] Levine BD. VO₂max: What do we know, and what do we still need to know? *J. Physiol.* 2008;586(1):25-34.
- [2] Mitchell JH, Sproule BJ, Chapman CB. The physiological meaning of the maximal oxygen intake test. *J Clin Invest* 1958;37(4):538-47.
- [3] Haykowsky M, Brubaker P, Kitzman D. Role of physical training in heart failure with preserved ejection fraction. *Curr Heart Fail Rep* 2012;9(2):101-6.
- [4] Kitzman DW, Little WC, Brubaker PH, Anderson RT, Hundley WG, Marburger CT, Brosnihan B, Morgan TM, Stewart KP. Pathophysiological characterization of isolated diastolic heart failure in comparison to systolic heart failure. *JAMA* 2002;288(17):2144-50.
- [5] Witte KK, Levy WC, Lindsay Ka, Clark AL. Biomechanical efficiency is impaired in patients with chronic heart failure. *Eur J Heart Fail* 2007;9(8):834-8.
- [6] Levy WC, Maichel Ba, Steele NP, Leclerc KM, Stratton JR. Biomechanical efficiency is decreased in heart failure during low-level steady state and maximal ramp exercise. *Eur J Heart Fail* 2004;6(7):917-26.
- [7] Neder JA, Nery LE, Andreoni S, Sachs A, Whipp BJ. Oxygen cost for cycling as related to leg mass in males and females, aged 20 to 80. *Int J Sports Med* 2000;21(4):263-9.
- [8] Lafortuna CL, Proietti M, Agosti F, Sartorio A. The energy cost of cycling in young obese women. *Eur J Appl Physiol* 2006;97(1):16-25.
- [9] Andersen P, Adams RP, Sjogaard G, Thorboe A, Saltin B. Dynamic knee extension as model for study of isolated exercising muscle in humans. *J Appl Physiol* 1985;59(5):1647-53.
- [10] Andersen P, Saltin B. Maximal perfusion of skeletal muscle in man. *J Physiol* 1985;366:233-49.
- [11] Koga S, Poole DC, Shiojiri T, Kondo N, Fukuba Y, Miura A, Barstow TJ. Comparison of oxygen uptake kinetics during knee extension and cycle exercise. *Am J Physiol Regul Integr Comp Physiol* 2005;288(1):R212-20.
- [12] Heinonen I, Saltin B, Kemppainen J, Sipilä HT, Oikonen V, Nuutila P, Knuuti J, Kalliokoski K, Hellsten Y. Skeletal muscle blood flow and oxygen uptake at rest and during exercise in humans: A pet study with nitric oxide and cyclooxygenase inhibition. *Am J Physiol Heart Circ Physiol* 2011;300(4):H1510-7.
- [13] Heinonen IH, Kemppainen J, Kaskinoro K, Peltonen JE, Borra R, Lindroos M, Oikonen V, Nuutila P, Knuuti J, Boushel R, Kalliokoski KK. Regulation of

human skeletal muscle perfusion and its heterogeneity during exercise in moderate hypoxia. *Am J Physiol Regul Integr Comp Physiol* 2010;299(1):R72-9.

[14] Lu H, Ge Y. Quantitative evaluation of oxygenation in venous vessels using T2-Relaxation-Under-Spin-Tagging MRI. *Magn Reson Med* 2008;60(2):357-63.

[15] Silvennoinen MJ, Clingman CS, Golay X, Kauppinen RA, van Zijl PC. Comparison of the dependence of blood R2 and R2* on oxygen saturation at 1.5 and 4.7 Tesla. *Magn Reson Med* 2003;49(1):47-60.

[16] Spees WM, Yablonskiy DA. Water proton MR properties of human blood at 1.5 Tesla: Magnetic susceptibility, T(1), T(2), T*(2), and non-Lorentzian signal behavior. *Magn Reson Med* 2001;45(2):333-42.

[17] Wright GA, Hu BS, Macovski A. Estimating oxygen saturation of blood in vivo with MR imaging at 1.5 T. *J Magn Reson Imaging* 1991;1(3):275-83.

[18] Qin Q, Grgac K, van Zijl PC. Determination of whole-brain oxygen extraction fractions by fast measurement of blood T(2) in the jugular vein. *Magn Reson Med* 2011;65(2):471-9.

[19] Zheng J, An H, Coggan AR, Zhang X, Bashir A, Muccigrosso D, Peterson LR, Gropler RJ. Noncontrast skeletal muscle oximetry. *Magn Reson Med* 2014;71(1):318-25.

[20] Elder CP, Cook RN, Chance MA, Copenhaver EA, Damon BM. Image-based calculation of perfusion and oxyhemoglobin saturation in skeletal muscle during submaximal isometric contractions. *Magn Reson Med* 2010;64(3):852-61.

[21] Lebon V, Carlier PG, Brillault-Salvat C, Leroy-Willig A. Simultaneous measurement of perfusion and oxygenation changes using a multiple gradient-echo sequence: application to human muscle study. *Magn Reson Imaging* 1998;16(7):721-9.

[22] Langham MC, Wehrli FW. Simultaneous mapping of temporally-resolved blood flow velocity and oxygenation in femoral artery and vein during reactive hyperemia. *J Cardiovasc Magn Reson* 2011;13:66.

[23] Langham MC, Jain V, Magland JF, Wehrli FW. Time-resolved absolute velocity quantification with projections. *Magn Reson Med* 2010;64(6):1599-606.

[24] Fernández-Seara Ma, Techawiboonwong A, Detre Ja, Wehrli FW. MR susceptometry for measuring global brain oxygen extraction. *Magn Reson Med* 2006;55(5):967-73.

[25] Haacke EM, Lai S, Reichenbach JR, Kuppusamy K, Hoogenraad FG, Takeichi H, Lin W. In vivo measurement of blood oxygen saturation using magnetic resonance imaging: a direct validation of the blood oxygen level-dependent concept in functional brain imaging. *Hum Brain Mapp* 1997;5(5):341-6.

- [26] Rodgers ZB, Jain V, Englund EK, Langham MC, Wehrli FW. High temporal resolution MRI quantification of global cerebral metabolic rate of oxygen consumption in response to apneic challenge. *J Cereb Blood Flow Metab* 2013;33(10):1514-22.
- [27] Wehrli FW, Rodgers ZB, Jain V, Langham MC, Li C, Licht DJ, Magland J. Time-resolved MRI oximetry for quantifying CMRO(2) and vascular reactivity. *Acad Radiol* 2014;21(2):207-14.
- [28] Fabry ME, San George RC. Effect of magnetic susceptibility on nuclear magnetic resonance signals arising from red cells: a warning. *Biochemistry* 1983;22(17):4119-25.
- [29] Jain V, Langham MC, Floyd TF, Jain G, Magland JF, Wehrli FW. Rapid magnetic resonance measurement of global cerebral metabolic rate of oxygen consumption in humans during rest and hypercapnia. *J Cereb Blood Flow Metab* 2011;31(7):1504-12.
- [30] Thulborn KR, Waterton JC, Matthews PM, Radda GK. Oxygenation dependence of the transverse relaxation time of water protons in whole blood at high field. *Biochim Biophys Acta* 1982;714(2):265-70.
- [31] Weisskoff RM, Kiihne S. MRI susceptometry: Image-based measurement of absolute susceptibility of MR contrast agents and human blood. *Magn Reson Med* 1992;24(2):375-83.
- [32] Jain V, Abdulmalik O, Propert KJ, Wehrli FW. Investigating the magnetic susceptibility properties of fresh human blood for noninvasive oxygen saturation quantification. *Magn Reson Med* 2012;68(3):863-7.
- [33] Langham MC, Magland JF, Floyd TF, Wehrli FW. Retrospective correction for induced magnetic field inhomogeneity in measurements of large-vessel hemoglobin oxygen saturation by MR susceptometry. *Magn Reson Med* 2009;61(3):626-33.
- [34] Schenck JF. The role of magnetic susceptibility in magnetic resonance imaging: MRI magnetic compatibility of the first and second kinds. *Med Phys* 1996;23(6):815-50.
- [35] Langham MC, Floyd TF, Mohler ER, Magland JF, Wehrli FW. Evaluation of cuff-induced ischemia in the lower extremity by magnetic resonance oximetry. *J Am Coll Cardiol* 2010;55(6):598-606.
- [36] Thompson RB, McVeigh ER. Real-time volumetric flow measurements with complex-difference MRI. *Magn Reson Med* 2003;50(6):1248-55.
- [37] Li C, Langham MC, Epstein CL, Magland JF, Wu J, Gee J, Wehrli FW. Accuracy of the cylinder approximation for susceptometric measurement of intravascular oxygen saturation. *Magn Reson Med* 2012;67(3):808-13.

- [38] Kety SS, Schmidt CF. The nitrous oxide method for the quantitative determination of cerebral blood flow in man; theory, procedure and normal values. *J Clin Invest* 1948;27(4):476-83.
- [39] Ozyener F, Rossiter HB, Ward SA, Whipp BJ. Influence of exercise intensity on the on- and off-transient kinetics of pulmonary oxygen uptake in humans. *J Physiol* 2001;533(Pt 3):891-902.
- [40] Esposito F, Mathieu-Costello O, Shabetai R, Wagner PD, Richardson RS. Limited maximal exercise capacity in patients with chronic heart failure: partitioning the contributors. *J Am Coll Cardiol* 2010;55(18):1945-54.
- [41] Jendzjowsky NG, Tomczak CR, Lawrance R, Taylor DA, Tymchak WJ, Riess KJ, Warburton DE, Haykowsky MJ. Impaired pulmonary oxygen uptake kinetics and reduced peak aerobic power during small muscle mass exercise in heart transplant recipients. *J Appl Physiol* (1985) 2007;103(5):1722-7.
- [42] Esposito F, Reese V, Shabetai R, Wagner PD, Richardson RS. Isolated quadriceps training increases maximal exercise capacity in chronic heart failure: the role of skeletal muscle convective and diffusive oxygen transport. *J Am Coll Cardiol* 2011;58(13):1353-62.
- [43] Chilibeck PD, Paterson DH, Cunningham DA, Taylor AW, Noble EG. Muscle capillarization O₂ diffusion distance, and VO₂ kinetics in old and young individuals. *J Appl Physiol* (1985) 1997;82(1):63-9.
- [44] van Beest PA, van der Schors A, Liefers H, Coenen LG, Braam RL, Habib N, Braber A, Scheeren TW, Kuiper MA, Spronk PE. Femoral venous oxygen saturation is no surrogate for central venous oxygen saturation. *Crit Care Med* 2012;40(12):3196-201.

Chapter 3: Discussion and Conclusions

Introduction and General Findings

All protocols and new techniques should be validated with a pilot study before they are utilized in a larger scale clinical patient study. The primary goal of the study in Chapter 2 that comprises the body of this thesis is to explore the feasibility and reproducibility of a new technique developed to simultaneously measure venous blood flow and oxygen saturation to in turn measure the oxygen extraction of working muscles during dynamic exercise with MRI.

To that end, we have developed a new MRI method to quantify in vivo blood flow, oxygen saturation, and oxygen consumption of a muscle during dynamic exercise and demonstrated the feasibility and reproducibility of the method with an imaging study on human volunteers. These physiological parameters are currently unavailable using noninvasive MRI techniques and have the potential to provide novel information about skeletal muscle function in diseased states such as heart failure.

Our measurements using the new technique are in good agreement with previously validated invasive study data (1). As well, the test-retest data showed statistically significant reproducibility for the new technique for blood flow, oxygen saturation, and oxygen consumption.. There are multiple limitations to the technique as currently developed, which are explored below. By addressing some of these limitations, we think that this new tool can help to elucidate individual impairments in the oxygen cascade, and help to develop recovery paths for patients with, and at-risk for, heart failure.

Limitations and Future Directions

The technique presented in Chapter 2 is robust, fast, and easy to integrate into standard clinical MRI protocols as it uses standard GRE and CD sequences already available on clinical scanners to make these measurements. There are

several limitations with the exercise imaging technique that should be explored in future development and studies.

A major limitation to exercise imaging is that MRI is extremely sensitive to movement; thus, the imaging protocol must commence immediately post-exercise, as opposed to during exercise. Additionally, as physiological parameters associated with exercise change rapidly following the cessation of exercise, the time between exercise cessation and starting imaging should be minimized.

Phase-dependent MRI techniques, such as complex-difference MRI and susceptometry, require sufficient mass of reference tissue surrounding the vessel of interest to correct for static phase variations. As well, susceptometry is dependent on vessel geometry and orientation (2). By focusing on a vessel segment parallel to the main magnetic field that can be approximated by an infinite cylinder, the quantification of susceptibility in the vessel, and thus oxygenation, is simplified. This condition naturally limits the set of vessels, and thus working muscle groups, which can be analyzed with the current technique, and may introduce a bias to the oxygen extraction (SvO_2 in particular) measurement depending on how well the approximation holds.

In addition, although regional venous blood flow was calculated, whether or not this femoral vein flow in fact corresponds exclusively to the exercising muscle tissue, or territory that the vein is draining, is not completely known. An understanding of the precise vessel draining system around the tissue of interest would allow for an accurate match of perfusion values in tissue with venous flow, and potentially extend the method to usability in additional areas.

An important next step in the future development of the proposed technique is to verify the ability of our measurements to detect true local changes in the tissue oxygen consumption. Also, the global changes to oxygen consumption would be interesting to compare with local changes, to assess how good of a surrogate whole body VO_2 measurement is for local muscle oxygen consumption.

Our method is proposed as an ideal candidate to investigate the progression of heart failure and the relationship between exercise intolerance and heart disease severity. A key clinical collaborator at the University of Alberta is the Alberta HEART study, which can further the progress on this technique and apply it to clinical populations.

Conclusions

Exercise training in heart failure could improve biomechanical efficiency. The study in Chapter 2 shows that it is feasible to measure blood flow and oxygen saturation simultaneously immediately post-exercise in the femoral vein, and the technique has good reproducibility. With these values, immediate post-exercise recovery of oxygen consumption to baseline values can be measured and modeled with an exponential decay curve. The time constant of this curve could be used as an endpoint metric in studies involving interventions such as exercise training or pharmaceutical agents including resveratrol.

Safe and robust methods to measure exercise capacity in disease states are needed to understand disease mechanisms and to evaluate treatment. Through development of these methods we can advance the state of medical understanding and provide people opportunities to live longer, healthier lives.

Chapter 3 References

[1] Andersen P, Saltin B. Maximal perfusion of skeletal muscle in man. *J Physiol* 1985;366:233-49.

[2] Langham MC, Magland JF, Epstein CL, Floyd TF, Wehrli FW. Accuracy and precision of MR blood oximetry based on the long paramagnetic cylinder approximation of large vessels. *Magnetic Resonance in Medicine* 2009;62(2):333-40.

Works Cited

Chapter 1 References

- [1] Levy WC, Maichel Ba, Steele NP, Leclerc KM, Stratton JR. Biomechanical efficiency is decreased in heart failure during low-level steady state and maximal ramp exercise. *European journal of heart failure* 2004;6(7):917-26.
- [2] Witte KK, Levy WC, Lindsay Ka, Clark AL. Biomechanical efficiency is impaired in patients with chronic heart failure. *European journal of heart failure* 2007;9(8):834-8.
- [3] Piña IL, Apstein CS, Balady GJ, Belardinelli R, Chaitman BR, Duscha BD, Fletcher BJ, Fleg JL, Myers JN, Sullivan MJ. Exercise and heart failure a statement from the american heart association committee on exercise, rehabilitation, and prevention. *Circulation* 2003;107(8):1210-25.
- [4] Balady GJ, Arena R, Sietsema K, Myers J, Coke L, Fletcher GF, Forman D, Franklin B, Guazzi M, Gulati M. Clinician's guide to cardiopulmonary exercise testing in adults a scientific statement from the american heart association. *Circulation* 2010;122(2):191-225.
- [5] Coronel R, De Groot J, Van Lieshout J. Defining heart failure. *Cardiovascular research* 2001;50(3):419-22.
- [6] Bui AL, Horwich TB, Fonarow GC. Epidemiology and risk profile of heart failure. *Nat Rev Cardiol* 2011;8(1):30-41.
- [7] Moe GW, Ezekowitz JA, O'Meara E, Howlett JG, Fremes SE, Al-Hesayen A, Heckman GA, Ducharme A, Estrella-Holder E, Grzeslo A. The 2013 canadian cardiovascular society heart failure management guidelines update: Focus on rehabilitation and exercise and surgical coronary revascularization. *Canadian Journal of Cardiology* 2014;30(3):249-63.
- [8] Ross H, Howlett J, Arnold JMO, Liu P, O'Neill B, Brophy J, Simpson C, Sholdice M, Knudtson M, Ross D. Treating the right patient at the right time: Access to heart failure care. *Canadian journal of Cardiology* 2006;22(9):749-54.
- [9] Arnold JMO, Liu P, Demers C, Dorian P, Giannetti N, Haddad H, Heckman GA, Howlett JG, Ignaszewski A, Johnstone DE. Canadian cardiovascular society consensus conference recommendations on heart failure 2006: Diagnosis and management. *Canadian Journal of Cardiology* 2006;22(1):23-45.
- [10] Tang, J. Quantification of Oxygen Saturation of Venous Vessels Using Susceptibility Mapping. McMaster University; 2012.

- [11] Billett, HH. Hemoglobin and Hematocrit. In: Walker, HK, Hall, WD, Hurst, JW, editors. *Clinical Methods: The History, Physical, and Laboratory Examinations*. Boston: Butterworth Publishers, a division of Reed Publishing; 1990.
- [12] Dominguez de Villota ED, Ruiz Carmona MT, Rubio JJ, de Andres S. Equality of the in vivo and in vitro oxygen-binding capacity of haemoglobin in patients with severe respiratory disease. *British journal of anaesthesia* 1981;53(12):1325-8.
- [13] Weber KT, Kinasewitz GT, Janicki JS, Fishman AP. Oxygen utilization and ventilation during exercise in patients with chronic cardiac failure. *Circulation* 1982;65(6):1213-23.
- [14] Gallagher P, Farrell A. 6 hematocrit and blood oxygen-carrying capacity. *Fish physiology* 1998;17:185-227.
- [15] Bassett D, Howley ET. Limiting factors for maximum oxygen uptake and determinants of endurance performance. *Medicine and science in sports and exercise* 2000;32(1):70-84.
- [16] Rowell LB, Taylor HL, Wang Y, Carlson WS. Saturation of arterial blood with oxygen during maximal exercise. *Journal of Applied Physiology* 1964;19(2):284-6.
- [17] Richardson RS, Knight DR, Poole DC, Kurdak SS, Hogan MC, Grassi B, Wagner PD. Determinants of maximal exercise VO₂ during single leg knee-extensor exercise in humans. *American Journal of Physiology-Heart and Circulatory Physiology* 1995;37(4):H1453.
- [18] Richardson R, Frank L, Haseler L. Dynamic knee-extensor and cycle exercise: Functional MRI of muscular activity. *International journal of sports medicine* 1998;19(03):182-7.
- [19] Arthur C. Guyton, JE. *Textbook of Medical Physics*. Philadelphia: Elsevier Inc.; 2006.
- [20] Ekblom B, Astrand PO, Saltin B, Stenberg J, Wallstrom B. Effect of training on circulatory response to exercise. *J Appl Physiol* 1968;24:518-528.
- [21] Williams JH, Powers SK, Stuart MK. Hemoglobin desaturation in highly trained athletes during heavy exercise. *Medicine and science in sports and exercise* 1986;18(2):168-73.

- [22] Pittman, RN. Chapter 7 Oxygen transport in normal and pathological situations: defects and compensations. In: Regulation of Tissue Oxygenation 2011.
- [23] Blomstrand E, Rådegran G, Saltin B. Maximum rate of oxygen uptake by human skeletal muscle in relation to maximal activities of enzymes in the krebs cycle. *The Journal of Physiology* 1997;501(Pt 2):455-60.
- [24] van Zijl PC, Eleff SM, Ulatowski JA, Oja JM, Ulug AM, Traystman RJ, Kauppinen RA. Quantitative assessment of blood flow, blood volume and blood oxygenation effects in functional magnetic resonance imaging. *Nature medicine* 1998;4(2):159-67.
- [25] Macmillan CS, Andrews PJ. Cerebrovenous oxygen saturation monitoring: Practical considerations and clinical relevance. *Intensive care medicine* 2000;26(8):1028-36.
- [26] West, JB. Pulmonary physiology and pathophysiology: an integrated, case-based approach. Lippincott Williams & Wilkins; 2007.
- [27] Jain V, Langham MC, Wehrli FW. MRI estimation of global brain oxygen consumption rate. *Journal of Cerebral Blood Flow & Metabolism* 2010;30(9):1598-607.
- [28] Langham MC, Wehrli FW. Simultaneous mapping of temporally-resolved blood flow velocity and oxygenation in femoral artery and vein during reactive hyperemia. *Journal of Cardiovascular Magnetic Resonance* 2011;13:66.
- [29] Andersen P, Saltin B. Maximal perfusion of skeletal muscle in man. *The Journal of Physiology* 1985(1985):233-49.
- [30] Armstrong WF, Zoghbi WA. Stress echocardiography: Current methodology and clinical applications. *Journal of the American College of Cardiology* 2005;45(11):1739-47.
- [31] Myers J, Gullestad L. The role of exercise testing and gas-exchange measurement in the prognostic assessment of patients with heart failure. *Current opinion in cardiology* 1998;13(3):145-55.
- [32] Myers J. Applications of cardiopulmonary exercise testing in the management of cardiovascular and pulmonary disease. *International journal of sports medicine* 2005;26(S 1):S49-55.
- [33] Ribeiro JP, Stein R, Chiappa GR. Beyond peak oxygen uptake: New prognostic markers from gas exchange exercise tests in chronic heart failure. *Journal of Cardiopulmonary Rehabilitation and Prevention* 2006;26(2):63-71.

- [34] Sullivan MJ, Knight J, Higginbotham M, Cobb F. Relation between central and peripheral hemodynamics during exercise in patients with chronic heart failure. muscle blood flow is reduced with maintenance of arterial perfusion pressure. *Circulation* 1989;80(4):769-81.
- [35] Myers J, Froelicher VF. Hemodynamic determinants of exercise capacity in chronic heart failure. *Annals of internal medicine* 1991;115(5):377-86.
- [36] Saltin AS. Cardiac output during submaximal and maximal work. 1964.
- [37] Saltin B. Hemodynamic adaptations to exercise. *The American Journal of Cardiology* 1985;55(10):D42-7.
- [38] Braden D, Carroll J. Normative cardiovascular responses to exercise in children. *Pediatric cardiology* 1999;20(1):4-10.
- [39] Hill AV, Lupton H. Muscular exercise, lactic acid, and the supply and utilization of oxygen. *Q J Med* 1923;16(62):135-71.
- [40] Casey DP, Joyner MJ. Skeletal muscle blood flow responses to hypoperfusion at rest and during rhythmic exercise in humans. *Journal of applied physiology* 2009;107(2):429-37.
- [41] Weber TF, von Tengg-Koblighk H, Kopp-Schneider A, Ley-Zaporozhan J, Kauczor H, Ley S. High-resolution phase-contrast MRI of aortic and pulmonary blood flow during rest and physical exercise using a MRI compatible bicycle ergometer. *European journal of radiology* 2011;80(1):103-8.
- [42] Cheng CP, Herfkens RJ, Taylor CA, Feinstein JA. Proximal pulmonary artery blood flow characteristics in healthy subjects measured in an upright posture using MRI: The effects of exercise and age. *Journal of Magnetic Resonance Imaging* 2005;21(6):752-8.
- [43] Langham MC, Magland JF, Epstein CL, Floyd TF, Wehrli FW. Accuracy and precision of MR blood oximetry based on the long paramagnetic cylinder approximation of large vessels. *Magnetic Resonance in Medicine* 2009;62(2):333-40.
- [44] Boushel R, Langberg H, Green S, Skovgaard D, Bülow J, Kjær M. Blood flow and oxygenation in peritendinous tissue and calf muscle during dynamic exercise in humans. *The Journal of physiology* 2000;524(1):305-13.
- [45] Kety SS. Measurement of regional circulation by the local clearance of radioactive sodium. *American heart journal* 1949;38(3):321-8.

- [46] Kety SS, Schmidt CF. The effects of altered arterial tensions of carbon dioxide and oxygen on cerebral blood flow and cerebral oxygen consumption of normal young men. *Journal of Clinical Investigation* 1948;27(4):484.
- [47] Kety SS, Schmidt CF. The nitrous oxide method for the quantitative determination of cerebral blood flow in man; theory, procedure and normal values. *Journal of Clinical Investigation* 1948;27(4):476-83.
- [48] Mayberg T, Lam A. Jugular bulb oximetry for the monitoring of cerebral blood flow and metabolism. *Neurosurgery clinics of North America* 1996;7(4):755-65.
- [49] Andersen P, Adams RP, Sjogaard G, Thorboe A, Saltin B. Dynamic knee extension as model for study of isolated exercising muscle in humans. *Journal of applied physiology* 1985;59(5):1647-53.
- [50] Coplin WM, O'Keefe GE, Grady MS, Grant GA, March KS, Winn HR, Lam AM. Thrombotic, infectious, and procedural complications of the jugular bulb catheter in the intensive care unit. *Neurosurgery* 1997;41(1):101-9.
- [51] Gill RW. Pulsed doppler with B-mode imaging for quantitative blood flow measurement. *Ultrasound in medicine & biology* 1979;5(3):223-35.
- [52] Hoskins P. Measurement of arterial blood flow by doppler ultrasound. *Clinical physics and physiological measurement* 1990;11(1):1.
- [53] Gill RW. Measurement of blood flow by ultrasound: Accuracy and sources of error. *Ultrasound in medicine & biology* 1985;11(4):625-41.
- [54] Eicke BM, Kremkau FW, Hinson H, Tegeler CH. Peak velocity overestimation and linear-array spectral doppler. *Journal of neuroimaging*. 1995;5(2):115-21.
- [55] Wesche J. The time course and magnitude of blood flow changes in the human quadriceps muscles following isometric contraction. *The Journal of physiology* 1986;377(1):445-62.
- [56] Walløe L, Wesche J. Time course and magnitude of blood flow changes in the human quadriceps muscles during and following rhythmic exercise. *The Journal of physiology* 1988;405(1):257-73.
- [57] Shoemaker J, Phillips S, Green H, Hughson R. Faster femoral artery blood velocity kinetics at the onset of exercise following short-term training. *Cardiovascular research* 1996;31(2):278-86.

- [58] Rådegran G. Ultrasound doppler estimates of femoral artery blood flow during dynamic knee extensor exercise in humans. *Journal of Applied Physiology* 1997;83(4):1383-8.
- [59] Daubeney PE, Pilkington SN, Janke E, Charlton GA, Smith DC, Webber SA. Cerebral oxygenation measured by near-infrared spectroscopy: Comparison with jugular bulb oximetry. *The Annals of thoracic surgery* 1996;61(3):930-4.
- [60] Van Beekvelt MC, Colier WN, Wevers RA, Van Engelen BG. Performance of near-infrared spectroscopy in measuring local O₂ consumption and blood flow in skeletal muscle. *Journal of Applied Physiology* 2001;90(2):511-9.
- [61] Jobsis FF. Noninvasive, infrared monitoring of cerebral and myocardial oxygen sufficiency and circulatory parameters. *Science (New York, N Y)* 1977;198(4323):1264-7.
- [62] Wahr JA, Tremper KK, Samra S, Delpy DT. Near-infrared spectroscopy: Theory and applications. *Journal of cardiothoracic and vascular anesthesia* 1996;10(3):406-18.
- [63] Nagdyman N, Fleck T, Schubert S, Ewert P, Peters B, Lange PE, Abdul-Khaliq H. Comparison between cerebral tissue oxygenation index measured by near-infrared spectroscopy and venous jugular bulb saturation in children. *Intensive care medicine* 2005;31(6):846-50.
- [64] Tortoriello TA, Stayer SA, Mott AR, Dean McKenzie E, Fraser CD, Andropoulos DB, Chang AC. A noninvasive estimation of mixed venous oxygen saturation using near-infrared spectroscopy by cerebral oximetry in pediatric cardiac surgery patients. *Pediatric Anesthesia* 2005;15(6):495-503.
- [65] Ito H, Ibaraki M, Kanno I, Fukuda H, Miura S. Changes in cerebral blood flow and cerebral oxygen metabolism during neural activation measured by positron emission tomography: Comparison with blood oxygenation level-dependent contrast measured by functional magnetic resonance imaging. *Journal of Cerebral Blood Flow & Metabolism* 2005;25(3):371-7.
- [66] Frackowiak RS, Lenzi GL, Jones T, Heather JD. Quantitative measurement of regional cerebral blood flow and oxygen metabolism in man using ¹⁵O and positron emission tomography: Theory, procedure, and normal values. *Journal of computer assisted tomography* 1980;4(6):727-36.
- [67] Mintun MA, Raichle ME, Martin WR, Herscovitch P. Brain oxygen utilization measured with O-15 radiotracers and positron emission tomography. *Journal of nuclear medicine : official publication, Society of Nuclear Medicine* 1984;25(2):177-87.

- [68] Ho SSY, Chan YL, Yeung DKW, Metreweli C. Blood flow volume quantification of cerebral ischemia: Comparison of three noninvasive imaging techniques of carotid and vertebral arteries. *American Journal of Roentgenology* 2002;178(3):551-6.
- [69] Spilt A, Box F, van der Geest RJ, Reiber JH, Kunz P, Kamper AM, Blauw GJ, van Buchem MA. Reproducibility of total cerebral blood flow measurements using phase contrast magnetic resonance imaging. *Journal of Magnetic Resonance Imaging* 2002;16(1):1-5.
- [70] Barhoum S, Rodgers ZB, Langham M, Magland JF, Li C, Wehrli FW. Comparison of MRI methods for measuring whole-brain venous oxygen saturation. *Magnetic Resonance in Medicine* 2014.
- [71] Hundley WG, Li HF, Hillis LD, Meshack BM, Lange RA, Willard JE, Landau C, Peshock RM. Quantitation of cardiac output with velocity-encoded, phase-difference magnetic resonance imaging. *The American journal of cardiology* 1995;75(17):1250-5.
- [72] Moran PR. A flow velocity zeugmatographic interlace for NMR imaging in humans. *Magnetic resonance imaging* 1982;1(4):197-203.
- [73] Axel L. Blood flow effects in magnetic resonance imaging. *American journal of roentgenology* 1984;143(6):1157-66.
- [74] Bryant D, Payne J, Firmin D, Longmore D. Measurement of flow with NMR imaging using a gradient pulse and phase difference technique. *Journal of computer assisted tomography* 1984;8(4):588-93.
- [75] Moran P, Saloner D, Tsui B. NMR velocity-selective excitation composites for flow and motion imaging and suppression of static tissue signal. *Medical Imaging, IEEE Transactions on* 1987;6(2):141-7.
- [76] Markl, M. *Velocity Encoding and Flow Imaging*. 2005.
- [77] Langham MC, Jain V, Magland JF, Wehrli FW. Time-resolved absolute velocity quantification with projections. *Magnetic resonance in medicine*. 2010;64(6):1599-606.
- [78] Gatehouse PD, Keegan J, Crowe LA, Masood S, Mohiaddin RH, Kreitner K, Firmin DN. Applications of phase-contrast flow and velocity imaging in cardiovascular MRI. *European radiology* 2005;15(10):2172-84.
- [79] O'Donnell M. NMR blood flow imaging using multiecho, phase contrast sequences. *Medical physics* 1985;12(1):59-64.

- [80] Dumoulin C, Souza S, Walker M, Wagle W. Three-dimensional phase contrast angiography. *Magnetic Resonance in Medicine* 1989;9(1):139-49.
- [81] Thompson RB, McVeigh ER. Real-time volumetric flow measurements with complex-difference MRI. *Magnetic Resonance in Medicine* 2003;50(6):1248-55.
- [82] Thulborn KR, Waterton JC, Matthews PM, Radda GK. Oxygenation dependence of the transverse relaxation time of water protons in whole blood at high field. *Biochimica et biophysica acta* 1982;714(2):265-70.
- [83] Gomori JM, Grossman RI, Yu-Ip C, Asakura T. NMR relaxation times of blood: Dependence on field strength, oxidation state, and cell integrity. *Journal of computer assisted tomography* 1987;11(4):684-90.
- [84] Wright GA, Hu BS, Macovski A. Estimating oxygen saturation of blood in vivo with MR imaging at 1.5 T. *Magnetic Resonance Imaging* 1991:275-83.
- [85] Oja JM, Gillen JS, Kauppinen RA, Kraut M, van Zijl PC. Determination of oxygen extraction ratios by magnetic resonance imaging. *Journal of Cerebral Blood Flow & Metabolism* 1999;19(12):1289-95.
- [86] Yablonskiy DA, Haacke EM. Theory of NMR signal behavior in magnetically inhomogeneous tissues: The static dephasing regime. *Magnetic Resonance in Medicine* 1994;32(6):749-63.
- [87] He X, Yablonskiy DA. Quantitative BOLD: Mapping of human cerebral deoxygenated blood volume and oxygen extraction fraction: Default state. *Magnetic Resonance in Medicine* 2007;57(1):115-26.
- [88] He X, Zhu M, Yablonskiy DA. Validation of oxygen extraction fraction measurement by qBOLD technique. *Magnetic Resonance in Medicine* 2008;60(4):882-8.
- [89] An H, Lin W. Quantitative measurements of cerebral blood oxygen saturation using magnetic resonance imaging. *Journal of Cerebral Blood Flow & Metabolism* 2000;20(8):1225-36.
- [90] An H, Lin W, Celik A, Lee YZ. Quantitative measurements of cerebral metabolic rate of oxygen utilization using MRI: A volunteer study. *NMR in Biomedicine* 2001;14(7-8):441-7.
- [91] An H, Lin W. Cerebral oxygen extraction fraction and cerebral venous blood volume measurements using MRI: Effects of magnetic field variation. *Magnetic resonance in medicine* 2002;47(5):958-66.

- [92] Yablonskiy DA, Haacke EM. An MRI method for measuring T2 in the presence of static and RF magnetic field inhomogeneities. *Magnetic resonance in medicine* 1997;37(6):872-6.
- [93] Yablonskiy DA, Reinius WR, Stark H, Haacke EM. Quantitation of T2' anisotropic effects on magnetic resonance bone mineral density measurement. *Magnetic resonance in medicine* 1997;37(2):214-21.
- [94] Chien D, Levin DL, Anderson CM. MR gradient echo imaging of intravascular blood oxygenation: T2* determination in the presence of flow. *Magnetic resonance in medicine* 1994;32(4):540-5.
- [95] Li D, Waight DJ, Wang Y. In vivo correlation between blood T2 and oxygen saturation. *Journal of Magnetic Resonance Imaging* 1998;8(6):1236-9.
- [96] Li D, Wang Y, Waight DJ. Blood oxygen saturation assessment in vivo using T2* estimation. *Magnetic resonance in medicine* 1998;39(5):685-90.
- [97] Sedlacik J, Rauscher A, Reichenbach JR. Quantification of modulated blood oxygenation levels in single cerebral veins by investigating their MR signal decay. *Zeitschrift für Medizinische Physik* 2009;19(1):48-57.
- [98] Sedlacik J, Reichenbach JR. Validation of quantitative estimation of tissue oxygen extraction fraction and deoxygenated blood volume fraction in phantom and in vivo experiments by using MRI. *Magnetic Resonance in Medicine* 2010;63(4):910-21.
- [99] Lu H, Ge Y. Quantitative evaluation of oxygenation in venous vessels using T2-relaxation-under-spin-tagging MRI. *Magnetic resonance in medicine* 2008;60(2):357-63.
- [100] Ogawa S, Lee TM, Kay AR, Tank DW. Brain magnetic resonance imaging with contrast dependent on blood oxygenation. *Proceedings of the National Academy of Sciences of the United States of America* 1990;87(24):9868-72.
- [101] Jain V, Abdulmalik O, Propert KJ, Wehrli FW. Investigating the magnetic susceptibility properties of fresh human blood for noninvasive oxygen saturation quantification. *Magnetic resonance in medicine* 2012;68(3):863-7.
- [102] Weisskoff RM, Kiihne S. MRI susceptometry: Image-based measurement of absolute susceptibility of MR contrast agents and human blood. *Magnetic Resonance in Medicine* 1992;24(2):375-83.
- [103] Haacke EM, Lai S, Reichenbach JR, Kuppusamy K, Hoogenraad FG, Takeichi H, Lin W. In vivo measurement of blood oxygen saturation using magnetic resonance imaging: A direct validation of the blood oxygen level-

dependent concept in functional brain imaging. *Human brain mapping* 1997;5(5):341-6.

[104] Liu Y, Pu Y, Fox PT, Gao J. Quantification of dynamic changes in cerebral venous oxygenation with MR phase imaging at 1.9 T. *Magnetic resonance in medicine* 1999;41(2):407-11.

[105] Langham MC, Magland JF, Floyd TF, Wehrli FW. Retrospective correction for induced magnetic field inhomogeneity in measurements of large-vessel hemoglobin oxygen saturation by MR susceptometry. *Magnetic resonance in medicine* 2009;61(3):626-33.

[106] Langham MC, Floyd TF, Mohler ER, Magland JF, Wehrli FW. Evaluation of cuff-induced ischemia in the lower extremity by magnetic resonance oximetry. *Journal of the American College of Cardiology* 2010;55(6):598-606.

[107] Li C, Langham MC, Epstein CL, Magland JF, Wu J, Gee J, Wehrli FW. Accuracy of the cylinder approximation for susceptometric measurement of intravascular oxygen saturation. *Magnetic resonance in medicine* 2012;67(3):808-13.

[108] Levitt, MH. *Spin dynamics: basic principles of NMR spectroscopy*. Wiley; 2001.

[109] Guyton AC, Hall J. *Textbook of medical physiology*. WB Saunder's Co., Philadelphia 2000;10th Edition.

[110] Jain V, Magland J, Langham M, Wehrli FW. High temporal resolution in vivo blood oximetry via projection-based T2 measurement. *Magnetic Resonance in Medicine* 2013;70(3):785-90.

[111] Foster EL, Arnold JW, Jekic M, Bender JA, Balasubramanian V, Thavendiranathan P, Dickerson JA, Raman SV, Simonetti OP. MR-compatible treadmill for exercise stress cardiac magnetic resonance imaging. *Magnetic Resonance in Medicine* 2012;67(3):880-9.

[112] Thavendiranathan P, Dickerson J, Scandling D, Balasubramanian V, Hall N, Foster E, Arnold JW, Pennell M, Simonetti OP, Raman SV. Myocardial function and perfusion assessment with exercise stress cardiovascular magnetic resonance using an MRI-compatible treadmill in patients referred for stress SPECT. *Journal of Cardiovascular Magnetic Resonance* 2012;14(Suppl 1):P1.

[113] Raymer GH, Allman BL, Rice CL, Marsh GD, Thompson RT. Characteristics of a MR-compatible ankle exercise ergometer for a 3.0 T head-only MR scanner. *Medical engineering & physics* 2006;28(5):489-94.

- [114] Ghomi RH, Bredella MA, Thomas BJ, Miller KK, Torriani M. Modular MR-compatible lower leg exercise device for whole-body scanners. *Skeletal radiology* 2011;40(10):1349-54.
- [115] Gusso S, Salvador C, Hofman P, Cutfield W, Baldi JC, Taberner A, Nielsen P. Design and testing of an MRI-compatible cycle ergometer for non-invasive cardiac assessments during exercise. *Biomedical engineering online* 2012;11:13.
- [116] Rossiter H, Ward S, Kowalchuk J, Howe F, Griffiths J, Whipp B. Effects of prior exercise on oxygen uptake and phosphocreatine kinetics during high-intensity knee-extension exercise in humans. *The Journal of Physiology* 2001;537(1):291-303.
- [117] Roest A, Lamb H, Van Der Wall E, Vliegen H, Van Den Aardweg J, Kunz P, De Roos A, Helbing W. Cardiovascular response to physical exercise in adult patients after atrial correction for transposition of the great arteries assessed with magnetic resonance imaging. *Heart* 2004;90(6):678-84.

Chapter 2 References

- [1] Levine BD. VO₂max: What do we know, and what do we still need to know? *J. Physiol.* 2008;586(1):25-34.
- [2] Mitchell JH, Sproule BJ, Chapman CB. The physiological meaning of the maximal oxygen intake test. *J Clin Invest* 1958;37(4):538-47.
- [3] Haykowsky M, Brubaker P, Kitzman D. Role of physical training in heart failure with preserved ejection fraction. *Curr Heart Fail Rep* 2012;9(2):101-6.
- [4] Kitzman DW, Little WC, Brubaker PH, Anderson RT, Hundley WG, Marburger CT, Brosnihan B, Morgan TM, Stewart KP. Pathophysiological characterization of isolated diastolic heart failure in comparison to systolic heart failure. *JAMA* 2002;288(17):2144-50.
- [5] Witte KK, Levy WC, Lindsay Ka, Clark AL. Biomechanical efficiency is impaired in patients with chronic heart failure. *Eur J Heart Fail* 2007;9(8):834-8.
- [6] Levy WC, Maichel Ba, Steele NP, Leclerc KM, Stratton JR. Biomechanical efficiency is decreased in heart failure during low-level steady state and maximal ramp exercise. *Eur J Heart Fail* 2004;6(7):917-26.
- [7] Neder JA, Nery LE, Andreoni S, Sachs A, Whipp BJ. Oxygen cost for cycling as related to leg mass in males and females, aged 20 to 80. *Int J Sports Med* 2000;21(4):263-9.
- [8] Lafortuna CL, Proietti M, Agosti F, Sartorio A. The energy cost of cycling in young obese women. *Eur J Appl Physiol* 2006;97(1):16-25.

- [9] Andersen P, Adams RP, Sjogaard G, Thorboe A, Saltin B. Dynamic knee extension as model for study of isolated exercising muscle in humans. *J Appl Physiol* 1985;59(5):1647-53.
- [10] Andersen P, Saltin B. Maximal perfusion of skeletal muscle in man. *J Physiol* 1985;366:233-49.
- [11] Koga S, Poole DC, Shiojiri T, Kondo N, Fukuba Y, Miura A, Barstow TJ. Comparison of oxygen uptake kinetics during knee extension and cycle exercise. *Am J Physiol Regul Integr Comp Physiol* 2005;288(1):R212-20.
- [12] Heinonen I, Saltin B, Kempainen J, Sipilä HT, Oikonen V, Nuutila P, Knuuti J, Kalliokoski K, Hellsten Y. Skeletal muscle blood flow and oxygen uptake at rest and during exercise in humans: A pet study with nitric oxide and cyclooxygenase inhibition. *Am J Physiol Heart Circ Physiol* 2011;300(4):H1510-7.
- [13] Heinonen IH, Kempainen J, Kaskinoro K, Peltonen JE, Borra R, Lindroos M, Oikonen V, Nuutila P, Knuuti J, Boushel R, Kalliokoski KK. Regulation of human skeletal muscle perfusion and its heterogeneity during exercise in moderate hypoxia. *Am J Physiol Regul Integr Comp Physiol* 2010;299(1):R72-9.
- [14] Lu H, Ge Y. Quantitative evaluation of oxygenation in venous vessels using T2-Relaxation-Under-Spin-Tagging MRI. *Magn Reson Med* 2008;60(2):357-63.
- [15] Silvennoinen MJ, Clingman CS, Golay X, Kauppinen RA, van Zijl PC. Comparison of the dependence of blood R2 and R2* on oxygen saturation at 1.5 and 4.7 Tesla. *Magn Reson Med* 2003;49(1):47-60.
- [16] Spees WM, Yablonskiy DA. Water proton MR properties of human blood at 1.5 Tesla: Magnetic susceptibility, T(1), T(2), T*(2), and non-Lorentzian signal behavior. *Magn Reson Med* 2001;542:533-42.
- [17] Wright GA, Hu BS, Macovski A. Estimating oxygen saturation of blood in vivo with MR imaging at 1.5 T. *J Magn Reson Imaging* 1991;1(3):275-83.
- [18] Qin Q, Grgac K, van Zijl PCM. Determination of whole-brain oxygen extraction fractions by fast measurement of blood T(2) in the jugular vein. *Magn Reson Med* 2011;65(2):471-9.
- [19] Zheng J, An H, Coggan AR, Zhang X, Bashir A, Muccigrosso D, Peterson LR, Gropler RJ. Noncontrast skeletal muscle oximetry. *Magn Reson Med* 2014;71(1):318-25.
- [20] Elder CP, Cook RN, Chance MA, Copenhaver EA, Damon BM. Image-based calculation of perfusion and oxyhemoglobin saturation in skeletal muscle during submaximal isometric contractions. *Magn Reson Med* 2010;64(3):852-61.
- [21] Lebon V, Carlier PG, Brillault-Salvat C, Leroy-Willig A. Simultaneous measurement of perfusion and oxygenation changes using a multiple gradient-

echo sequence: application to human muscle study. *Magn Reson Imaging* 1998;16(7):721-9.

[22] Langham MC, Wehrli FW. Simultaneous mapping of temporally-resolved blood flow velocity and oxygenation in femoral artery and vein during reactive hyperemia. *J Cardiovasc Magn Reson* 2011;13:66.

[23] Langham MC, Jain V, Magland JF, Wehrli FW. Time-resolved absolute velocity quantification with projections. *Magn Reson Med* 2010;64(6):1599-606.

[24] Fernández-Seara Ma, Techawiboonwong A, Detre Ja, Wehrli FW. MR susceptometry for measuring global brain oxygen extraction. *Magn Reson Med* 2006;55(5):967-73.

[25] Haacke EM, Lai S, Reichenbach JR, Kuppusamy K, Hoogenraad FG, Takeichi H, Lin W. In vivo measurement of blood oxygen saturation using magnetic resonance imaging: a direct validation of the blood oxygen level-dependent concept in functional brain imaging. *Hum Brain Mapp* 1997;5(5):341-6.

[26] Rodgers ZB, Jain V, Englund EK, Langham MC, Wehrli FW. High temporal resolution MRI quantification of global cerebral metabolic rate of oxygen consumption in response to apneic challenge. *J Cereb Blood Flow Metab* 2013;33(10):1514-22.

[27] Wehrli FW, Rodgers ZB, Jain V, Langham MC, Li C, Licht DJ, Magland J. Time-resolved MRI oximetry for quantifying CMRO(2) and vascular reactivity. *Acad Radiol* 2014;21(2):207-14.

[28] Fabry ME, San George RC. Effect of magnetic susceptibility on nuclear magnetic resonance signals arising from red cells: a warning. *Biochemistry* 1983;22(17):4119-25.

[29] Jain V, Langham MC, Floyd TF, Jain G, Magland JF, Wehrli FW. Rapid magnetic resonance measurement of global cerebral metabolic rate of oxygen consumption in humans during rest and hypercapnia. *J Cereb Blood Flow Metab* 2011;31(7):1504-12.

[30] Thulborn KR, Waterton JC, Matthews PM, Radda GK. Oxygenation dependence of the transverse relaxation time of water protons in whole blood at high field. *Biochim Biophys Acta* 1982;714(2):265-70.

[31] Weisskoff RM, Kiihne S. MRI susceptometry: Image-based measurement of absolute susceptibility of MR contrast agents and human blood. *Magn Reson Med* 1992;24(2):375-83.

[32] Jain V, Abdulmalik O, Propert KJ, Wehrli FW. Investigating the magnetic susceptibility properties of fresh human blood for noninvasive oxygen saturation quantification. *Magn Reson Med* 2012;68(3):863-7.

- [33] Langham MC, Magland JF, Floyd TF, Wehrli FW. Retrospective correction for induced magnetic field inhomogeneity in measurements of large-vessel hemoglobin oxygen saturation by MR susceptometry. *Magn Reson Med* 2009;61(3):626-33.
- [34] Schenck JF. The role of magnetic susceptibility in magnetic resonance imaging: MRI magnetic compatibility of the first and second kinds. *Med Phys* 1996;23(6):815-50.
- [35] Langham MC, Floyd TF, Mohler ER, Magland JF, Wehrli FW. Evaluation of cuff-induced ischemia in the lower extremity by magnetic resonance oximetry. *J Am Coll Cardiol* 2010;55(6):598-606.
- [36] Thompson RB, McVeigh ER. Real-time volumetric flow measurements with complex-difference MRI. *Magn Reson Med* 2003;50(6):1248-55.
- [37] Li C, Langham MC, Epstein CL, Magland JF, Wu J, Gee J, Wehrli FW. Accuracy of the cylinder approximation for susceptometric measurement of intravascular oxygen saturation. *Magn Reson Med* 2012;67(3):808-13.
- [38] Kety SS, Schmidt CF. The nitrous oxide method for the quantitative determination of cerebral blood flow in man; theory, procedure and normal values. *J Clin Invest* 1948;27(4):476-83.
- [39] Ozyener F, Rossiter HB, Ward SA, Whipp BJ. Influence of exercise intensity on the on- and off-transient kinetics of pulmonary oxygen uptake in humans. *J Physiol* 2001;533(Pt 3):891-902.
- [40] Esposito F, Mathieu-Costello O, Shabetai R, Wagner PD, Richardson RS. Limited maximal exercise capacity in patients with chronic heart failure: partitioning the contributors. *J Am Coll Cardiol* 2010;55(18):1945-54.
- [41] Jendzjowsky NG, Tomczak CR, Lawrance R, Taylor DA, Tymchak WJ, Riess KJ, Warburton DE, Haykowsky MJ. Impaired pulmonary oxygen uptake kinetics and reduced peak aerobic power during small muscle mass exercise in heart transplant recipients. *J Appl Physiol* (1985) 2007;103(5):1722-7.
- [42] Esposito F, Reese V, Shabetai R, Wagner PD, Richardson RS. Isolated quadriceps training increases maximal exercise capacity in chronic heart failure: the role of skeletal muscle convective and diffusive oxygen transport. *J Am Coll Cardiol* 2011;58(13):1353-62.
- [43] Chilibeck PD, Paterson DH, Cunningham DA, Taylor AW, Noble EG. Muscle capillarization O₂ diffusion distance, and VO₂ kinetics in old and young individuals. *J Appl Physiol* (1985) 1997;82(1):63-9.
- [44] van Beest PA, van der Schors A, Liefers H, Coenen LG, Braam RL, Habib N, Braber A, Scheeren TW, Kuiper MA, Spronk PE. Femoral venous oxygen

saturation is no surrogate for central venous oxygen saturation. Crit Care Med 2012;40(12):3196-201.

Chapter 3 References

[1] Andersen P, Saltin B. Maximal perfusion of skeletal muscle in man. J Physiol 1985;366:233-49.

[2] Langham MC, Magland JF, Epstein CL, Floyd TF, Wehrli FW. Accuracy and precision of MR blood oximetry based on the long paramagnetic cylinder approximation of large vessels. Magnetic Resonance in Medicine 2009;62(2):333-40.